

Spring 2012

# Unified knowledge model for stability analysis in cyber physical systems

Tamal Paul



**Department:**

# UNIFIED KNOWLEDGE MODEL FOR STABILITY ANALYSIS IN CYBER PHYSICAL SYSTEMS

by

TAMAL PAUL

A THESIS

Presented to the Faculty of the Graduate School of

MISSOURI UNIVERSITY OF SCIENCE AND TECHNOLOGY

In Partial Fulfillment of the Requirements for the Degree

MASTER OF SCIENCE IN ELECTRICAL ENGINEERING

2012

Approved by

Dr. Jonathan W. Kimball, Advisor
Dr. Badrul H. Chowdhury
Dr. Mariesa L. Crow

# ABSTRACT

The amalgamation and coordination between computational processes and physical components represent the very basis of cyber-physical systems. A diverse range of CPS challenges had been addressed through numerous workshops and conferences over the past decade. Finding a common semantic among these diverse components which promotes system synthesis, verification and monitoring is a significant challenge in the cyber-physical research domain. Computational correctness, network timing and frequency response are system aspects that conspire to impede design, verification and monitoring. The objective of cyber-physical research is to unify these diverse aspects by developing common semantics that span each aspect of a CPS.

The work of this thesis revolves around the design of a typical smart grid-type system with three PV sources built with PSCAD®[1]. A major amount of effort in this thesis had been focused on studying the system behavior in terms of stability when subjected to load fluctuations from the PV side. The stability had been primarily reflected in the frequency of the generator of the system. The concept of droop control had been analyzed and the parameterization of the droop constant in the shape of an invariant forms an essential part of the thesis as it predicts system behavior and also guides the system within its stable restraints.

As an extension of a relationship between stability and frequency, the present study goes one step ahead in describing the sojourn of the system from stability to instability by doing an analysis with the help of tools called Lyapunov-like functions. Lyapunov-like functions are, for switched systems, a class of functions that are used to measure the stability for non linear systems. The use of Lyapunov-like functions to judge the stability of this system had been tested and discussed in detail in this thesis and simulation results provided.

[1]PSCAD® is a registered trademark of Manitoba HVDC Research Center Inc.

# ACKNOWLEDGMENT

To have completed this thesis, I owe the deepest sense of gratitude to my advisor Dr. Jonathan W. Kimball for his constant support, intellectual advice and inspiration. I am deeply indebted to him for taking time out of his busy schedule and providing me intellectual support as well as financial support thereby making it possible for me to come up with this work. I am truly grateful that I could work under his aegis since the time I was admitted to Missouri University of Science and Technology for the Masters program.

I am also extremely grateful to Dr. Bruce McMillin, Dr. Maciej Zawodniok and Dr. Keith Corzine for their invaluable support and academic guidance. I would also like to thank the Intelligent Systems Center and the Energy Research and Development Center at Missouri S&T for their support of this project.

I would especially like to thank Thomas Roth, my project partner for his excellent contribution to our research group and my thesis. No measure of thanks can do justice to his excellent contribution towards the 'smart' communication between PSCAD® sockets which helped me set up the test bed to run experiments and prove my results and corroborate my theoretical analysis with practical simulations.

Also I would like to extend a special note of thanks to Dr. Badrul Chowdhury and Dr. Mariesa Crow, Department of Electrical and Computer Engineering for graciously consenting to be on my thesis committee, taking their valuable time out of their busy schedule to review my thesis and for being such excellent course instructors.

No work is ever complete without the blissful mental support and love of one's family. In that context I would like to thank my mother, Mrs Gitul Pal; my father, Mr Goutam Pal, the best parents that one could have for being the pillars of motivation and encouragement for me to tide me over thick and thin. Also a special vote of thanks to my cousin Sangeeta Sur and Subhendu Pal for always being there with me. I am immensely thankful for the level of love and emotional support that they had bestowed upon me throughout my Masters program abroad.

# TABLE OF CONTENTS

# LIST OF ILLUSTRATIONS

# LIST OF TABLES

# 1. INTRODUCTION

## 1.1. BACKGROUND

A Cyber-Physical System (CPS) is an engineered physical system which consists of interacting distributed cyber and physical components. A CPS typically consists of a multitude of interacting distributed components. CPSs are often deployed in critical applications like advanced electric power systems, automated aircraft systems, intelligent highway systems, automated factories and smart houses. Unintended or misunderstood interactions among the CPS components might cause unwanted/unpredictable behavior thereby leading to serious consequences. Therefore it is imperative to develop approaches to ensure that both hardware and software components can integrate their operations into the system without interference or unanticipated interactions.

Often CPS failures occur when various subsystems are designed and tested in isolation and then integrated. Each subsystem may have been designed to meet the given specifications, but not to meet unforeseen circumstances arising from their combination. A car is designed for speeds between 0 and 100 mph. We certainly wouldn't want the steering to lock up or the brakes to fail at speeds greater than 100 mph, or fail if the car goes backwards. Luckily, today's automobiles have over one hundred years of design experience, so failures in cars are uncommon. However, as these systems become Cyber-Physical, they do not have such long histories. Modern cars contain over 10 million lines of code often developed separately for individual components [1]. This complexity can lead to unintended interactions. In 2005, CNN reported on the Toyota Prius where it stalled without warning due to reaching an ambiguous state between regions of operation. Avoiding situations such as this is why it is important to overlay a system-level scientific approach to CPS integration.

The engineering life cycle represents the steps of constructing a system. The key challenge in engineering a CPS is representing and merging fundamentally different subsystem aspects along the engineering life cycle as illustrated in Figure 1.1.

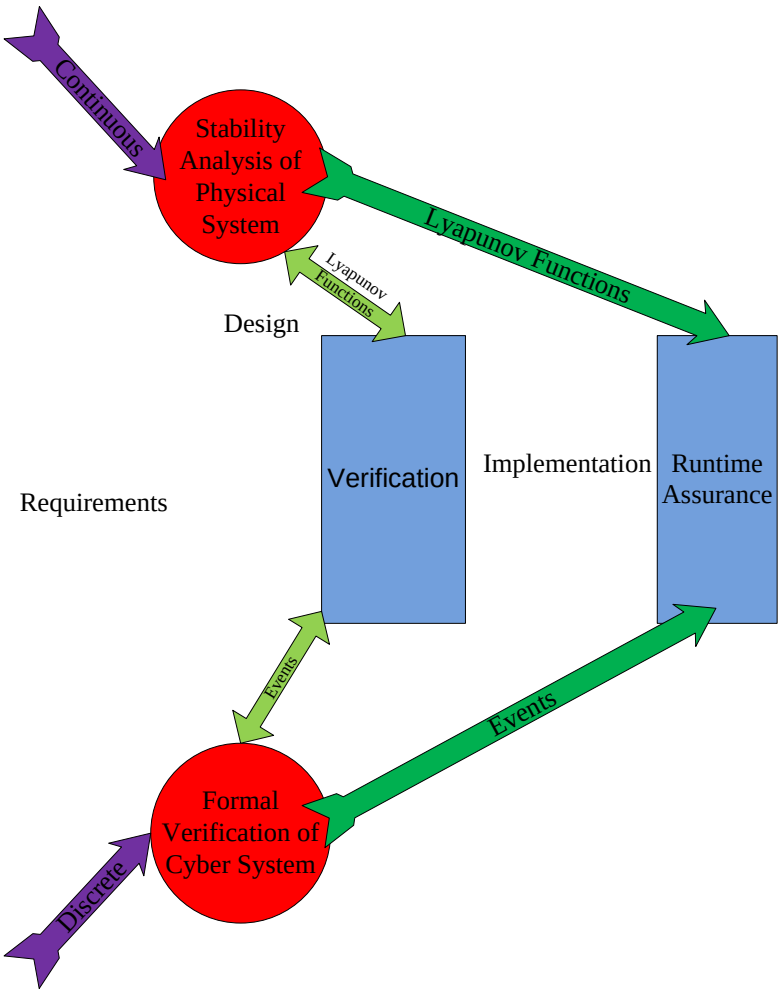


Figure 1.1. The Science behind the engineering of a CPS

## 1.2. LITERATURE REVIEW

The tight conjoining of and coordination between computational resources and physical components represents the core of cyber-physical systems (CPS) research [2]. A wide variety of CPS challenge problems have been identified through numerous workshops over the last decade. Universally common to cyber-physical systems are three principal functional components, a (distributed) cyber component, a networking/communications component, and an underlying physical infrastructure. So

integration, correctness, and stability are significant challenges in creating the tight conjoining of these three components.

For a CPS, cyber subsystems are naturally represented by discrete states and the physical subsystems are represented by continuous functions. The work of this thesis merges discrete events from the cyber subsystems with continuous events of the physical subsystems described by Lyapunov functions [3].

The current design approaches focus on separate components of a system. For example, a Lyapunov-based design of a closed loop controller for a physical system typically assumes hard-real-time limits on communication and processing delay. Again, the traditional real-time networks focus on providing service with fixed performance limits, for example CAN, FlexRay.

However a complex, distributed system-of-systems, such as the power grid or an electric vehicle, would challenge such traditional and standalone design approaches. A large network with hundreds of devices would require significant over-engineering to guarantee typical, conservative delays for a control loop. Traditional control-theory based approaches assume uninterrupted communication in the loop with low delays. Moreover, a typical Lyapunov-based stability analysis requires a monotonous convergence towards a desired operating state. This is achieved by requiring a negative (definite) first difference of a Lyapunov function candidate. In general, that means that the system will monotonically converge to the desired state. However, often the physical system can accommodate a disruption, bounded in time and magnitude, when a Lyapunov-like function may increase. Furthermore, controllers are traditionally designed to accommodate the worst-case scenario, that is, largest change/deviations/disturbance on all degrees-of-freedom. A proper design will always involve a fail-proof approach to handle erroneous situations, such as a short-circuiting of power lines.

For the physical aspect of a CPS, switched system analysis techniques can be used [4]. Cyber-physical systems can be modeled with a variety of abstractions, including hybrid automata and timed I/O automata [5]. Both of these automata types capture the dual aspects of the systemdiscrete dynamics that reflect the cyber changes and continuous dynamics to model the physical system. However, analysis tools for these formulations are challenging to use or, for some systems, non-existent.

Instead, a switched system models just the continuous dynamics, while allowing for mode changes due to some external action. That is, the cyber aspect of the system is modeled separately and only its impact on the physical system is incorporated. The main advantage of this approach is the partitioning of the problem. Switched system analysis, using Lyapunov or Lyapunov-like functions [6–8], can identify switching sequences that are allowable and switching sequences that cause instability. The switching sequences may be restricted in the state space or, for more generality, in the time domain. Timing restrictions (both maximum and minimum) can then be mapped into constraints for tools native to the cyber domain that determine whether the cyber controller meets stability requirements.

A unifying framework for designing cyber-physical systems is desired; however, the problem lies in the absence of any comprehensive tool to do so. The crucial point missing is a semantically common method of relating cyber, network, and physical actions and dynamics. However some work is path breaking in this direction. Acumen [9] bridges the gap between analytic models and simulation codes. Invariants and predicate transformers on the state of CPS was explored for dynamical systems in [10] and more recently in [11] which gives a formalism for invariant interaction and incremental invariant composition. The interaction of invariants for purely cyber processes, has its origins in [12] which affords composition of sequential proofs governed by the property of noninterference.

An invariant, essentially, is a logical predicate on a system state that does not change its truth value if satisfied by the system execution. An axiomatic basis for the truth of invariants on cyber systems was first proposed by [13]. In this system, program actions are related to logical truth through axioms and inference rules. Invariants are widely used ranging from algorithm instruction [14] to never claims in model checking. Invariants are well-understood for cyber processes, but extending them into the network and physical domains requires some insight.

From the physical perspective, as described in [3], Lyapunov functions can be applied to describe the dynamics of the physical system. Lyapunov functions can describe the complex behavior of a power grid [15]. However, there are no definite ways to find a Lyapunov function for nonlinear systems. In a switched system, a substitute (proxy) of a true Lyapunov function can be found by using either the

norm of the state vector or the energy of the system (the latter being used in the present work). Under certain conditions, this may be termed a Lyapunov-like function [6] and can verify the stability characteristics of the system.

Lyapunov functions have also been used to describe network stability [16–18]. Conceptually, Lyapunov-like functions can be constructed by modeling network traffic as a control feedback problem and then bounding the number and timing of outstanding messages and/or acknowledgements.

Authors in [19] have shown that advanced electric power grid is a complex real-time with both cyber and physical components. The interaction between two otherwise properly functioning individual components might result in an interference. The main type of incorrectness discussed in this paper is in the frequency domain. The authors used RT-PROMELA to construct the model and then checked it with RT-SPIN. To reduce the problem of state explosion, the model was decomposed into several other sub-models, each with a smaller state space that could be checked individually.

An architecture for a future electric power distribution system had been discussed in [20] which is widely used for for plug-and play of distributed renewable energy and distributed energy storage devices. The architecture described in this paper was proposed by the NSF FREEDM Systems Center, Raleigh, NC, as a roadmap for a future automated and flexible electric power distribution system. In the envisioned BEnergy Internet, a system that enables flexible energy sharing is proposed for consumers in a residential distribution system. The principal technologies needed to promote this vision had been discussed by the authors of this paper in addition with the FREEDM Systems Center.

An initiative to amalgamate the smart grid with Distributed Grid Intelligence (DGI) to manage the distribution and storage of renewable energy had been undertaken in [21]. This is also a work sponsored by the FREEDM systems center. DGI uses distributed algorithms in a novel way to attain economically feasible utilization and storage of alternative energy sources in a distributed fashion. These Intelligent Energy Management (IEM) nodes coordinate among themselves to effectively and economically manage their power generation, utility and storage. The authors of this paper had discussed key aspects in the implemenation of such schemes and outlined

preliminary results obtained by the integration of the proposed approach with a functional SST model used in FREEDM. This paper basically shows the effect of "smart" technology on a local grid and its advantages.

Authors in [22] presents proof rules as an extension of Hoare's Communicating Sequential Processes [23]. The rules deal with total correctness; all programs terminate in the absence of deadlock. The commands sent and received are treated symmetrically, simplifying the rules and allowing send to appear in guards. The work also discusses sufficient conditions for showing that a program is deadlock-free. The usage of the technique had been demonstrated by an elaborate example.

The appropriateness behind the application of Lyapunov-like functions is particularly interesting while studying the dynamics of interconnected cyber-phyical systems. In the context of switched systems, the basic concept of vector Lyapunov functions [24] can be considered,and also expanded to include Lyapunov-like functions. Vector Lyapunov functions have been previoulsy used to analyze jump non-linear systems [25], a class of systems with certain common fetaures with switched systems where the switching is driven by a Markov random process.

Lyapunov-like functions can also be used to analyze discrete-time systems with multiple time scales. These functions can be used to determine whether the updates occur frequently enough, but not too frequently [26] so as to safeguard stability. But then again single perturbation methods [27] allow the analysis of each time scale to focus on a subset of the state variables.

Thus for a CPS, each controller usually has complete information about a small portion of the complete physical system but limited information about the interface between this small physical sub-system and the rest of the system, and infrequently-updated information about other cyber-physical subsystems. Thus even if a particular subsystem is stable, forming a true Lyapunov function is almost impossible especially for a non-linear system.

Therefore the focus needs to be shifted towards Lyapunov-like functions along with a proper understanding of Lyapunov and Lyapunov-like systems. This is why the present study focuses on a Lyapunov-like approach and its justifiable implementaion in the context of an interconnected system. The following subsection describes the proposed approach that would be adopted to study a complex cyber-physical system

with the aid of Lyapunov-like tools since as had been substantiated before, designing Lyapunov-like functions for such a non linear system is virtually impossible.

## 1.3. PROPOSED APPROACH

Cyber-Physical Systems (CPS) consist of distributed computation interconnected by computer networks that monitor and control switched physical entities interconnected by physical infrastructures [2]. In the emerging smart grid, for example, system state provides input into distributed computer algorithms that manage power and energy via local computation with messaging passing over a computer network collectively resulting in control signals to advanced power electronics. This thesis seeks to unify the knowledge present in these diverse aspects through developing common semantics that span each aspect of a CPS. Specifically, a smart grid type system had been considered. Power commands to various loads and alternative energy sources are stepped in response to cyber controllers that are networked. This thesis shows the development of a physical invariant, based on the theory of Lyapunov-like functions, and a cyber invariant, that governs the correctness of a power dispatch algorithm, and couples the two to develop an overall system stability invariant. The invariant approach is tested with a set of simulations. The system stability had been reflected in the generator frequency. The frequency variations in the switched system in response to cyber commands had been captured. Also a non-interfering droop law had been proposed to preserve the stability of the system. The Lyapunov-like function that describes this behavior is derived from the error in the system energy. This function also gives an estimate of the system stability which is also a major part of this thesis. Simulations had been carried out to show the Lyapunov-like behavior of the system and thus predict the overall system stability.

The present thesis is a follow up from the paper presented in the KASTLES SOCA 2011 conference [2]. The author of this thesis is also one of the authors of the aforementioned paper presented in the KASTLES conference. An introduction to the dynamics of a switched system and the application of Lyapunov and Lyapunov-like functions in such systems have been discussed in Section 2. The physical/power electronic model of the experimental system have been described in Section 3 along with its control strategy. Section 3 also describes the cyber control strategy adopted

for this work which involves the “Intelligent” communication between the DGI s and their power balancing algorithm. Power simulation experiments have been discussed in Section 4 . Section 4 concludes with an introduction to the Droop Theory. This had been taken up in Section 5 which discusses droop analysis and reports subsequent simulations conducted. Section 5 also covers the correlation between invariant theory and droop analsyis. Experiments reported in this chapter primarily show the successful amalgamation of invariant prediction and simulation results. This can be described as the most important section of this thesis as the experimental results convey the message of the author and substantiates the theoretical analysis. The final section (Section 6) discusses the conclusions and the future work that can be done as an extension of this present study.

# 2. SWITCHED SYSTEM THEORY

## 2.1. INTRODUCTION

A switched system is a fundamentally continuous-time system with changes that occur at discrete times [4]. The study of a bouncing ball provides a classic example to describe the dynamics of a switched system: its dynamics are governed by gravity and Newton's laws of motion, and its velocity changes (instantaneously, as approximated) direction when it hits a surface. In this particular ball example, the switching instants are externally imposed but they might also be related to the system dynamics. A switched system is distinguished from a hybrid system in that discrete state dynamics are not modeled. Switched system analysis can identify switching sequences that are permissible and switching sequences that cause instability. The switching sequences may be restricted in the state space or in the time domain.

The continuous state of the system can be expressed as a vector of state variables ($\mathbf{x} \in \mathbb{R}^n$) whose values describe the system at a given time, and whose time history describe the system dynamics from the initial conditions to the current time. The inputs, expressed as a vector $\mathbf{u}$, may be external to the system or generated with feedback of a combination of the state variables and outputs. The outputs, expressed as the vector $\mathbf{y}$, are the only measurable characteristics of the system. The state-space formulation of a system, for some (possibly nonlinear) vector-valued functions $\mathbf{f}(\cdot)$ and $\mathbf{g}(\cdot)$ and some initial condition $\mathbf{x}_0$ on $\mathbf{x}$ at time $t_0$, is

$$\frac{d\mathbf{x}}{dt} = \mathbf{f}(\mathbf{x}, \mathbf{u}), \tag{1}$$

$$\mathbf{y} = \mathbf{g}(\mathbf{x}, \mathbf{u}), \tag{2}$$

$$\mathbf{x}\,(t_0) = \mathbf{x}_0 \tag{3}$$

## 2.2. LYAPUNOV AND LYAPUNOV-LIKE FUNCTIONS

A well-known tool for stability analysis of an autonomous continuous system (that is, one with no external inputs $\mathbf{u}$) is a *Lyapunov function*, $V(\mathbf{x})$. A Lyapunov

function has the following properties:

1. $V(\mathbf{x})$ is positive definite, that is, $V(\mathbf{x}) > 0 \ \forall \mathbf{x} \neq 0, V(0) = 0$.

2. $V(\mathbf{x})$ is radially unbounded.

3. $\frac{dV}{dt} \leq 0$ along all trajectories ($\frac{\partial V}{\partial x}\mathbf{f}(\mathbf{x}) \leq 0$).

If $\frac{dV}{dt}$ is non-positive, the system is stable. If $\frac{dV}{dt}$ is strictly negative, the system is asymptotically stable.

Unfortunately, while finding Lyapunov functions for low-order linear systems is relatively straightforward, finding Lyapunov functions for higher order systems pose enormous computational challenges and burden. As a matter of fact, there are no general techniques for finding Lyapunov functions for non-linear systems. For switched systems, another class of functions may be considered, namely *Lyapunov-like* functions [6–8]. A Lyapunov-like function must be positive definite and radially unbounded, just like a Lyapunov function. However, its derivative need not be negative at all times. Instead, we are only concerned with its value at isolated points. Multiple Lyapunov-like functions may be used for different operating modes.

We can consider a switched system that may operate in several different modes, enumerated by $k$. For each mode, it is possible to define a Lyapunov-like function $V_k(\mathbf{x}_k)$. If the system switches between modes, the only values of $V_k(\mathbf{x}_k)$ that matter are the values when the $k^{th}$ mode becomes active. If those values form a decreasing or non-increasing series, and the same holds true for all admissible values of $k$, then the switched system is stable. This concept is shown conceptually in Figure 2.1.

## 2.3. LYAPUNOV AND LYAPUNOV-LIKE FUNCTIONS IN A CPS

For switched discrete time linear systems, a switching law can be proposed which is dependant on system state with a dwell time designed to ensure asymptotic stability for the entire system [28]. A significant characteristic of Lyapunov-like functions is that they may not be monotonically decreasing in both time as well as state driven instants . Thus it made possible for the authors of [28] to come up with a stabilizing switching law having a lower switching frequency in contrast with recent results. Also it was shown that the proposed switching law ensured that a bounded perturbation

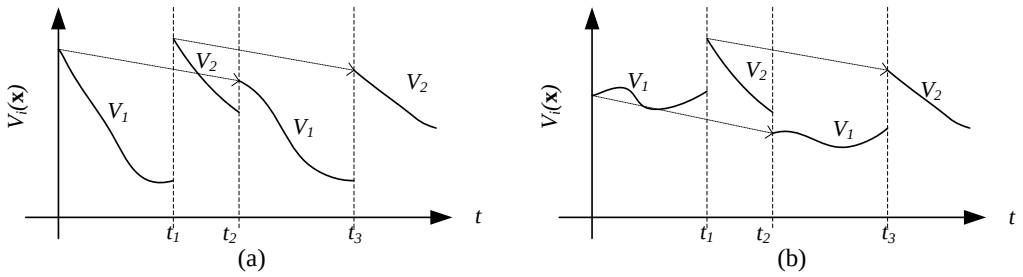


Figure 2.1. Asymptotic stability using multiple Lyapunov functions ($V_1$ and $V_2$). (a) Two true Lyapunov functions. (b) One Lyapunov function ($V_2$), one Lyapunov-like function ($V_1$).

implied bounded states. Feedback principles can be also used in designing switching laws. As in [29], a state feedback stabilizing switching law with dwell time had been developed for switched discrete-time linear systems. When compared with switching laws without time-driven switching laws, the former can reduce switching frequency. Also [29] goes on to show that the system state is bounded under the proposed switching laws if the given system is perturbed by a bounded perturbation.

The authors in [30] identify two types of stabilizability for switched systems: the pointwise stabilizability and the consistent stabilizability. This paper depicts the necessary conditions and sufficient conditions for both types in the context of switched linear systems.

Authors in [31] had addressed the problem of switched state feedback stabilization in switched linear systems with exponential uncertainties. Exponential uncertainties involve terms like $e^{mr}$ which is dependant on an unknown time varying parameter $r$. The design for such exponentially uncertain models from the control system point of view is pretty onerous. In the context of such an equivalent switched model, the switching strategy and associated state feedback controllers had been designed so that such switched model is asymptotical stabilization based on switched Lyapunov function technology.

Lyapunov functions had also been adopted to sample discrete switching events in cyber-physical systems. An event driven control methodology that employs Lyapunov sampling had been applied by the authors of [32] to networked control systems. A theoretical guideline had been presented to apply the Lyapunov sampling to a set of

closed loop systems sharing a serial bus line. Emphasis had been laid on recognizing requirements that need to be met to guarantee overall stability. An effective implementation approach had been presented for the controlled area network in addition to addressing problems due to the implicit distributed architecture of the NCS [32].

Not enough emphasis can be stressed on the challenges posed on providing integrity, efficiency and satisfactory performance for evolving cyber-physical systems [33]. Commendable work had been done in this paper by providing a Simplex Architecture which incorporates a supervisory controller that takes corrective measure only when the system is in potential danger of violating an important invariant property. The key factor in determining the switching control logic is that it should guarantee safe/stable system operation at all possible operating instants without being unduely conservative. Past work had involved composing Lyapunov functions for the underlying continuos dynamical system. For instance in order to verify a decision module in a system with continuos dynamics, a Lyapunov function's stability region can be used to drive the decision module [34]. A Lyapunov function for a controller for a particular plant defines an n-dimensional ellipsoid within an n-dimensional state space where, if the current system state is within the ellipsoid and the controller is used, the system will converge to a setpoint. If a Lyapunov function exists for the safety controller where the stability region is defined within the operational constraints without containing property violation states, and we know the maximum gradient over time for any controller within the Lyapunov stability region, it is possible to formally derive the decision module switching rule. If the current system state is at least the maximum gradient times the control iteration time away from the Lyapunov stability region boundary, the complex controller can be used. In the worst case, the state space will proceed at the maximum gradient towards the Lyapunov stability region boundary, but will not cross it before the next control iteration. It is then possible to switch to the safety controller which is guaranteed to converge to the setpoint without leaving the Lyapunov stability region. Thus the property violation region is never entered as had been explained in [33].

Thus Lyapunov-like functions are powerful tools for the analysis of a complex CPS. The present scope of work seeks to use the energy of the error as a Lyapunov-like function. It is important to note that the error should be measured with respect to a

certain desired physical operating point. Thus for each operating mode of the physical sub-system, a Lyapunov-like function can be defined, such as the energy in the error in all the state variables [2]. Then, as the cyber system state evolves, the Lyapunov-like functions can be checked. The derivative of the Lyapunov-like functions can be monitored and used to determine minimum and maximum times between switching instants. The study can be focused on a single scalar function of the state variables instead of considering the various dynamics of those state variables.

# 3. CYBER-PHYSICAL CONTROLS

## 3.1. PHYSICAL SYSTEM DESCRIPTION

The model described in this thesis is basically a "smart-grid" type system which consists of a generator and three converters (all in three phase) and operating in a grid-connected mode to absorb/inject power as governed by a cyber dispatch algorithm from the external finite-inertia generator [2]. Thus the converters can function either as rectifiers or as inverters. One of the aims of the present study is to operate the system in a stable domain. The stable operation of the system depends on the commanded power pulses and the dwell time between the perturbation instants.

The physical system was simulated in PSCAD® as illustrated in Figure 3.1. As can be seen, there are three converters ( all in three phase) interacting among themseleves, connected by lines with reasonable impedance and eventually connected to a generator by a transformer. Two of the converters inject power (source) into the grid and thus behave as inverters. The third converter acts as a rectifier and deliver power out of the grid (load). The switching strategy for the converter operation had been framed according to the desired control strategy which is to produce as much power as commanded by the cyber dispatch algorithm.

## 3.2. CONVERTER SWITCHING CONTROLS

The control strategy adopted for the converter switching action has been represented in the block diagram representation in Figure 3.2. The relationship between the active and reactive power transfer in the simulated system can be expressed in the $d-q$ reference frame [35] as

$$P = \frac{3}{2}(V_q I_q + V_d I_d) \tag{4}$$

$$Q = \frac{3}{2}(V_q I_d - V_d I_q) \tag{5}$$

In (4)-(5), $V_q$ and $I_q$ are the $q$-axis voltages and currents while $V_d$ and $I_d$ are the $d$-axis voltages and currents. The converter $a-b-c$ currents $(I_a, I_b, I_c)$ are converted into

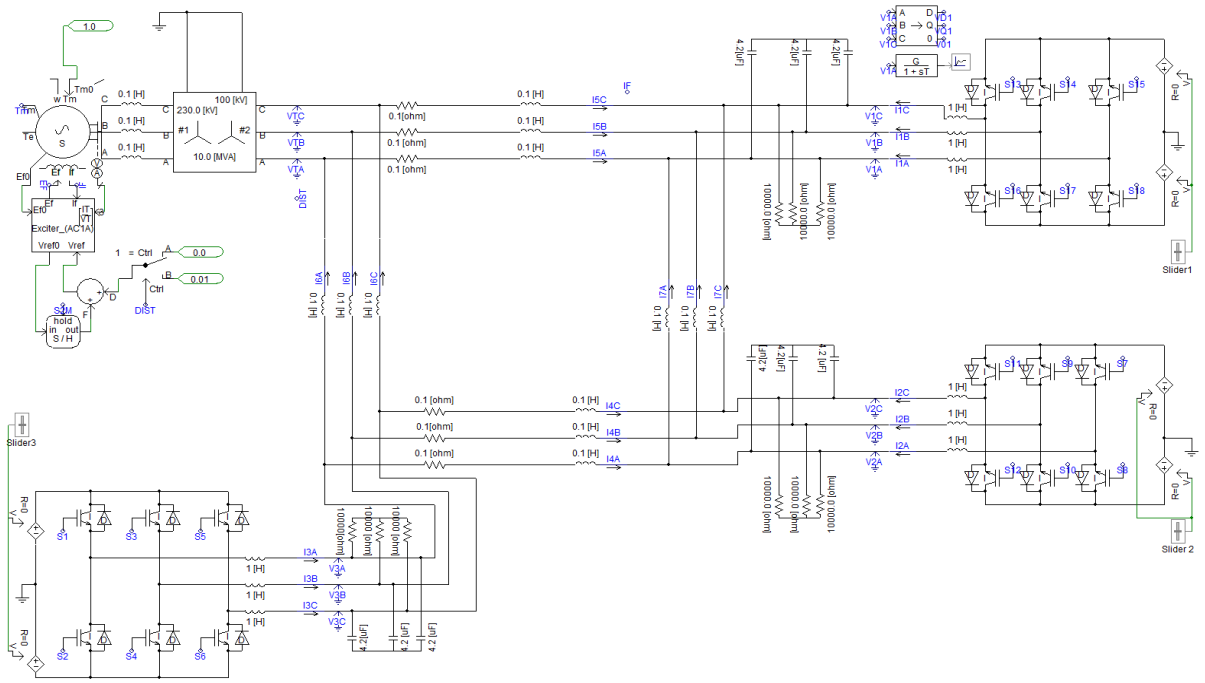


Figure 3.1. Physical System Representation simulated in PSCAD®.

their respective $d$ and $q$ counterparts. The cyber algorithm delivers the commanded values of $P$ and $Q$. Depending upon the commanded values of $P^*$ and $Q^*$, it is possible to calculate the ideal $d$ and $q$ axis currents for each converter as shown in the following pair of equations.

$$I_d^* = 2(P^* V_d + Q^* V_q) \tag{6}$$

$$I_q^* = 2(P^* V_q - Q^* V_d) \tag{7}$$

In (6)-(7), $P^*$ and $Q^*$ are the commanded values of active and reactive powers from the cyber algorithm. In the present thesis, the commanded value of reactive power is always zero for simplicity.

The ideal $d$ and $q$ axis currents are converted back to their respective $a-b-c$ counterparts. The control mechanism involved in this thesis is current regulated control or Hysteresis control. Therefore delta modulation is imposed to control the

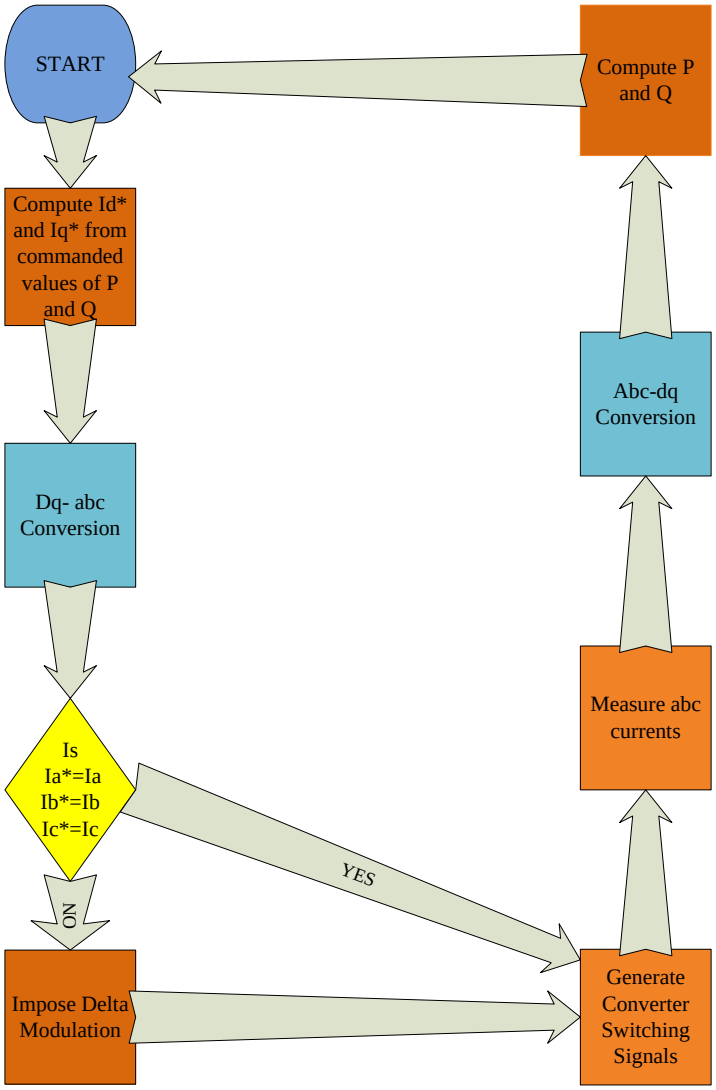


Figure 3.2. Block diagram representation of the converter switching scheme algorithm.

converter currents to the desired $a-b-c$ current values. This generates the switching signals for the converters.

Thus the ideal $I_a$, $I_b$, $I_c$ can be converted back to their respective ideal $d-q$ counterparts. According to (4)-(5), these ideal currents will generate the commanded values of active and reactive power at nominal operating system voltage and frequency conditions. Not shown in Figure 3.2 is a phase-locked loop that determines the system frequency to be used in the $abc-dq$ conversion. Typically a phase lock loop (PLL) is a control system that generates an output signal whose phase is related to the

phase of an input reference signal. This is thus the switching strategy devised for the present system which predominantly uses reference frame theory and current based control scheme.

### 3.3. SYSTEM ARCHITECTURE

Let us consider the FREEDM architecture as discussed in [20] and illustrated in Figure 3.3. FREEDM forms a microgrid of energy storage (DESD) energy resources (DRER), and LOADs to share power for the good of the entire system. This can be envisioned as a future smart distribution system. There are intelligent flow controllers (Nodes) which contain physical actuators (Solid State Transformers (SSTs)) for controllingl power flow to and from a shared electrical bus, under direction of cooperating Distributed Grid Intelligence Processes ($DGIs$).

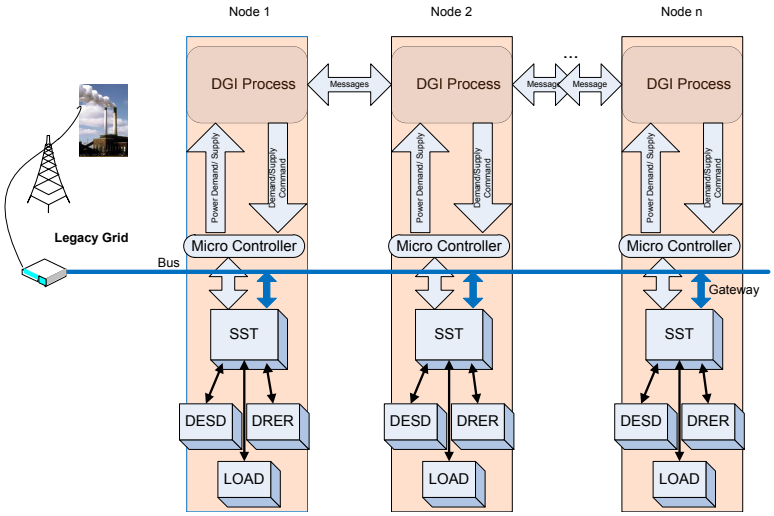


Figure 3.3. FREEDM Power Management Architecture [21]

It can be assumed that each Node is potentially owned and located in a house or business. Within each Node, the $DGI$ processes compute a power cost and use a drafting process [36]. Drafting is a receiver-initiated load-balancing procedure; if a Node (S) has available power generation capacity, it solicits bids from loaded Nodes (L). This introduces a whole new concept of power migration which is bound to have

some effect on the system dynamics. This interaction between power migration and system dynamics is very important and will be the crux of our analysis in the next subsection.

### 3.4. LYAPUNOV-LIKE ANALYSIS OF THE SYSTEM

The following section has an analytical approach towards the study of a simple system where a pair of FREEDM nodes connected to a power grid are communicating over a network. It is to be noted that the power flow on the grid is otherwise internally balanced. The two nodes ($S$ and $L$) communicate in such a way such that $L$ requests one quantum of power $\delta$ from $S$. Nothing happens if $S$ fails to receive this message from $L$. However in the possible event that $S$ does receive its intended message, it increases its power output by $\delta$ and sends an acknowledgment to $L$. After $L$ receives a valid acknowledgement, it increases its load by $\delta$. Messages are then sent at a rate of $\lambda$ and received at a rate of $\mu$ (after accounting for transit time and queueing), for an average delay time $R_d$ as described below. During mode I, $S$ is actively migrating power and $\lambda \geq \mu$. For a brief time at the beginning of the communication process, $\mu = 0$ due to the transit time. The delay time and queueing may result in power perturbations.

It is possible to model the dynamics of the average number of messages from $S$ to $L$ that have been sent but not received, $K$, as per the equation shown below

$$\frac{dK}{dt} = \lambda - \mu \tag{8}$$

where $K \geq 0$ by definition. Therefore, the net error in power (i.e., the difference between the source power and the load power) is $P_{error} = \delta K$. This net error will tend to increase the grid frequency, which is governed by a simplified swing equation,

$$\frac{d\omega}{dt} = -\frac{V_1 V_2}{J\omega X} sin(\theta - \theta_0) - \frac{D}{J}(\omega - \omega_0) + \frac{P_{err}}{J\omega} - \frac{kP^2}{J\omega} \tag{9}$$

where $D$ is the natural damping due to frequency-sensitive loads and $J$ is the effective rotational inertia. Here $V_1$ is the generator back emf, $V_2$ is the bus voltage at the generator terminals, $\theta - \theta_0$ represents the torque angle, and $k$ is power scaling factor that encapsulates the voltage and resistance and scales the gross power in terms of

power loss. If a large enough error persists, the frequency will become too high. When this condition is detected, the system must switch to mode II, in which $S$ no longer migrates additional quanta but instead follows a droop law of the form $P_S = P_{request} - m(\omega - \omega_0)$. During mode II, $\lambda = 0$ but $\mu \geq 0$ because $L$ may continue to process messages in its queue of received messages. After switching modes at $t_{II}$, the net error in the power will be proportional to the number of messages that are still outstanding $K$, less the droop effect, so $P_{error}(t) = \delta K - m(\omega - \omega_0)$.

The decision whether to switch from mode I to mode II may be determined based on some metric of the system state. A potential Lyapunov-like function is a quadratic in the two dynamic variables,

$$V(\omega, \theta) = \frac{J}{2}(\omega - \omega_0)^2 + \frac{V_1 V_2}{\omega X}(1 - cos(\theta - \theta_0)). \tag{10}$$

$$\frac{dV}{dt} = J(\omega - \omega_0)\frac{d\omega}{dt} + \frac{V_1 V_2}{\omega X}(sin(\theta - \theta_0)\frac{d\theta}{dt} \tag{11}$$

Substituting (9) in (11)

$$\frac{dV}{dt} \quad = \quad J(\omega - \omega_0)[-\frac{D}{J}(\omega - \omega_0) + \frac{\delta K}{J\omega} - \frac{m}{J\omega}(\omega - \omega_0) - \frac{kP^2}{J\omega}]$$

This derivative must be negative for the function to be a Lyapunov-function. Therefore,

$$\left\{I_{P1} : (\omega - \omega_0)^2(D\omega + m) + (\omega - \omega_0)(kP^2) > (\omega - \omega_0)(\delta K)\right\} \tag{12}$$

This parameterization of the droop constant gives us our invariant that guides the system within its stable restraints. For all values of $m$ obeying the above invariant,the system must be stable. This equation can be solved further to obtain the droop constant in the droop control in terms of the system parameters as expressed in equation:

$$m > \frac{\delta K - kP^2}{\omega - \omega_0} - D\omega \tag{13}$$

The absence of $\theta - \theta_0$ in the final invariant expression makes the proposed approach invariant independent of a generator. Thus it was possible to derive an invariant which would guide the system behavior. The crucial challenge was integrating the cyber controls and study the effects of the cyber controls on the invariant that has been framed from the physical structure of the model. Experimental results reported in the upcoming section will prove the accuracy of this invariant in terms of system behavior and simulation results.

## 3.5. CYBER CONTROLS

This section is adopted from the work published in [2] to give the readers an understanding of how the physical system gets governed by the cyber algorithm and also the principle behind the mechanism of cyber physical controls. The author of this thesis would like to thank his research group co-advisor Dr. Bruce McMillin, Department of Computer Science, Missouri University of Science and Technology and his research partner Thomas P. Roth, Department of Computer Science, Missouri University of Science and Technology for thier invaluable contribution behind this chapter. This section basically describes the conjoining of the physical model with the cyber domain.

**3.5.1. Cyber Algorithm.** $I_{P1}$ does not fully govern the overall stability of the system. As the cyber algorithm PowerBalance's [21] commands operate on the power system electronics, its actions are asynchronous with respect to those of the power electronics. Therfore it can be concluded that the power balancing algorithm has the ability to interfere with the truth of the invariant $I_{P1}$.

In the cyber power management algorithm each of $n$ processes executes an algorithm triggered by the state of the underlying power system, either $high$ or $low$. At all times the system should maintain the invariant $\{I_{C1} : n\nu + \sum_l^n high_l + \sum_l^n low_l = g\}$ (where $\nu$ is the nominal load per Node, $high_l$ and $low_l$ are the amount of variance above and below the nominal load and $g$ is a measure of the excess amount of draw or supply to/from a grid-type connection). This algorithm approximates a distributed solution to the fractional knapsack problem [21]. The fractional knapsack problem requires the invariant $\{I_{C2} : \exists_{l,m} max\ high_l^r - max\ high_m^{r+1} < 0, r = 0, ...., k-1\}$ (where $high^r$ indicates the $r^{th}$ decision made by the algorithm. The function $migrate(\delta, j)$

is a command to the underlying power system to provide/accept a quantum of power to/from a Node $j$.

The invariant $I_{C2}$ holds at termination of the algorithm, by the greedy choice principle. Due to lack of strict synchronization between cyber processes, assignment $low_i = low_i + \delta$ potentially interferes with the truth of the invariant $I_{C1}$. Potentially, $k$ migrations are outstanding at any point in time. Thus, the invariant is relaxed to $I'_{C1}$ until the migration has been received at process $P_j$:

$\{Q'_{C1}/I'_{C1} : \{n\nu + \sum_l^n high_l + k\delta + \sum_l^n low_l = g\}$

Since, in this model, when a rendezvous occurs at the select message, this modified invariant becomes true in the receiving process (by the rule of satisfaction [22]).

For the cyber-physical system under study, the conjunction of the cyber invariant and a logical statement related to the physical system stability gives the final invariant. Analysis of the physical system can be done with a Lyapunov or Lyapunov-like function. If we are concerned only with asymptotic stability, in this case, we must remain in mode II at all times and use $I_{P1}$ directly. Otherwise, $\dot{V}$ may be positive.

If *boundedness* is sufficient, then the following invariant is appropriate:

$$\{I_P : I_{P1} \vee (V(\omega, K) < V_{bound}) \vee (V(t) < V(t_{II}))\} \tag{14}$$

where $V_{bound}$ is the maximum allowable value of $V$, $V(t)$ is the value of $V(\omega, P_{error})$ at the present time and $V(t_{II})$ is its value at the most recent previous switch over to mode II.

The Lyapunov invariant (12) provides a relationship between the amount of frequency error and the number of pending/dropped migrations. To ensure that the actions of the $A_1 : P_j!select$ and $A_2 : low_i = low_i + \delta$ do not interfere with $I'_{C1}$. $\{I'_{C1} \wedge I_P\}A_1\{I_P \wedge I_N\}$ holds as a theorem when $k = K$, thus, bounding the cyber invariant by the Lyapunov invariant. To guarantee the CPS maintains the invariant, the system invariant is added as a guard, $I'_{C1} \wedge I_P \wedge I_N$, as a weakest precondition on the communication. This can be shown in the form of a cyber algorithm [2] written in a CSP-like language [23].

**3.5.2. Integration of Physical and Cyber Systems.** PSCAD® talks to the cyber algorithms through a C++ socket interface. Send and receive functions

were written to handle the transfer of arrays with arbitrary but known lengths. These functions were called through FORTRAN, the language embedded in PSCAD®. The send function allowed PSCAD® to transfer merged data to an external controller coded in C++, while the receive function probed for controller responses that could be imported back into the PSCAD® environment.

Two PSCAD® components were designed to encapsulate the C socket code: `pscad_send` and `pscad_recv`. The `pscad_send` component took an $n$-dimension line as an input which was created through combining multiple data signals . Its parameters specified the IP address of the external cyber control and a time offset $R_d$ of the delay between each transmission. During runtime, `pscad_send` transmitted the current state of its associated signals to the given address once every $R_d$ simulation seconds.

The `pscad_recv` component provided an $n$-dimension line as an output which was data tapped to access individual signals. Its output contained the most recent set of signals obtained from an external program tasked with controlling the simulation. During runtime, `pscad_recv` updates its output line with the most recent set of received data. Figure 3.4 shows the actual implementation of these components in the PSCAD® environment, where the input of `pscad_send` corresponds to $x(t)$ and the output of `pscad_recv` corresponds to $x(t+1)$.

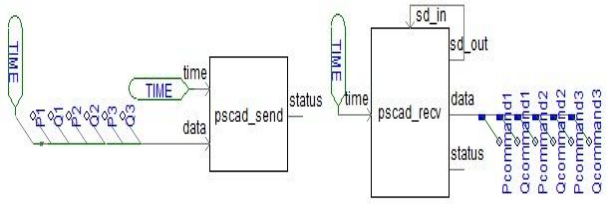


Figure 3.4. Integration of cyber components in the PSCAD® environment.

The basic experimental setup consisted of manipulated traces of the PowerBalance C++ code resulting from sequences of inputs $x(t)$ producing an output $x(t+1)$ as a vector of power migrations. PSCAD® provided the input as the most recent

snapshot of power settings for the three converters, specified as an array in the form $x(t) = \{t, P1(t), Q1(t), P2(t), Q2(t), P3(t), Q3(t)\}$. These are parameterized by $t$ (time) representing the latency involved in the PowerBalance algorithm computation. The migrate power commands for the converters were dispatched to PSCAD® in the form $x(t+1) = \{P1C, Q1C, P2C, Q2C, P3C, Q3C\}$.

For experiments in the present study, the external controller mapped simulation time to a set of power changes in the form $m(t) = \{1, dP1, dQ1, dP2, dQ2, dP3, dQ3\}$. The basic architecture of the `pscad_send` and `pscad_recv` components is illustrated in Figure 3.5.

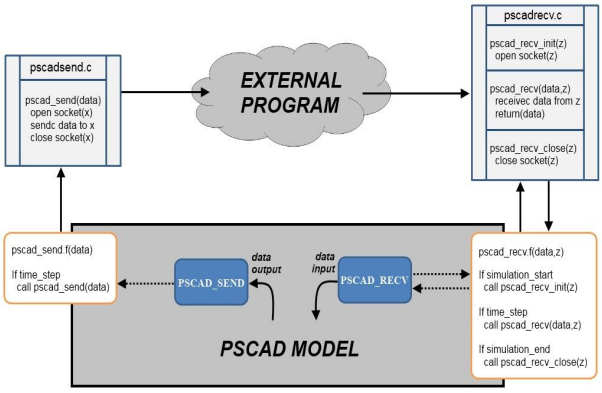


Figure 3.5. Communicating Architecture of the PSCAD® model with the external environment.

# 4. STABILITY ANALYSIS EXPERIMENTS

## 4.1. FREQUENCY MONITORING AND STABILITY ANALYSIS

The simulations have been carried out in PSCAD®. The power pulses were commanded by the cyber control at each converter end to emulate the power migration discussed in Section 3.4.

In Fig. 4.1 a state of the system has been described when the system is forced into an unusual state (one that does not satisfy the cyber invariant $I'_{C1}$ through a series of switched system states that result in unbalanced power migrations. In Table 4.1, the system is forced to remain in Mode I (only cyber commands control the system) while contents of each row at 0.8 s and 0.9 s do not sum to zero causing a variation in the frequency domain (Figure 4.1. Even at time 1.0 s, when $I'_{C1}$ becomes satisfied (by guarding the migration to reduce excess power transfers), the combined system invariant $I'_{C1} \wedge I_P \wedge I_N$ is still invalidated. The reason is that the proposed Lyapunov-like function is not strong enough to *recover* from frequency instability without switching to a different system mode. The error in energy for the system is very important since it becomes the Lyapunov-like function and hence our tool to ascertain stability.

The Lyapunov-like function that describes this behavior is derived from the error in the system energy (15):

$$V = \Delta E = \frac{J}{2}(\omega - \omega_0)^2 + \frac{V_1 V_2}{\omega X}(1 - cos(\theta - \theta_0)). \tag{15}$$

Table 4.1. Switched cyber system states resulting in unbalanced power migrations.

| **Time** | **SST 1** | **SST 2** | **SST 3** |
|---|---|---|---|
| 0.0 | 0 | 0 | 0 |
| 0.8 | 10 | 0 | 0 |
| 0.9 | 10 | -20 | 0 |
| 1.0 | 20 | 0 | -20 |

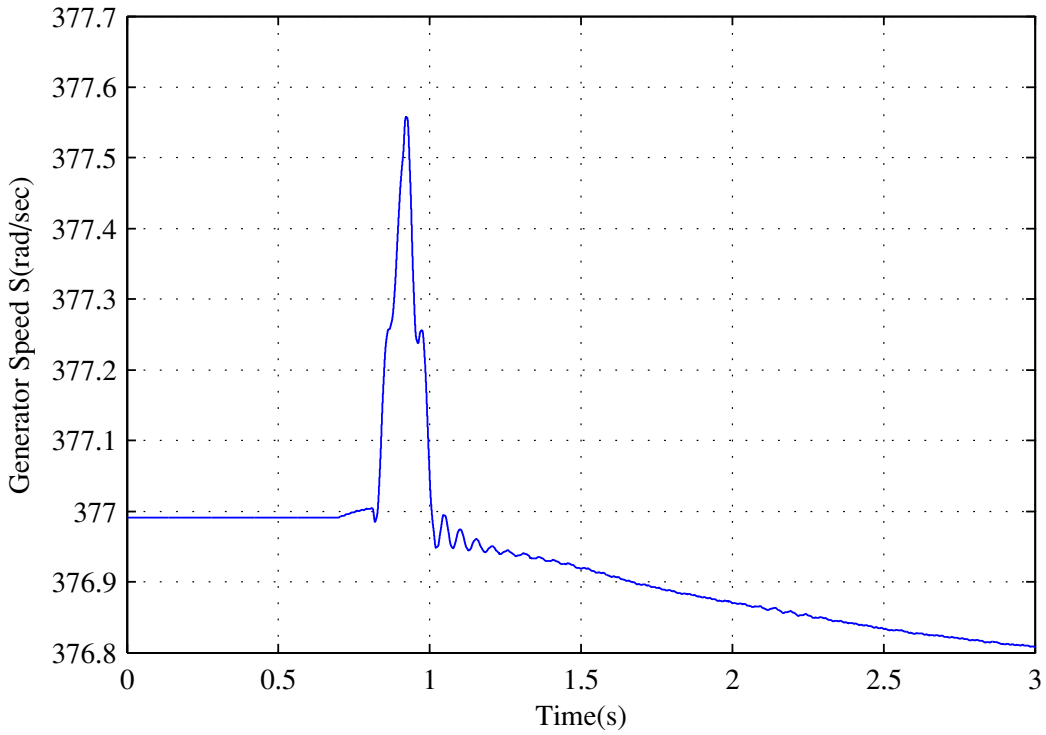


Figure 4.1. Frequency variations in switched system response with only cyber correction

where $J$ is the inertia constant of the system. $\omega$ is the angular frequency at which the system operates and $\omega_0$ is the nominal frequency of 60 Hz at steady state level. $V_1$ is the generator back emf, $V_2$ is the bus voltage at the generator terminals, $\theta - \theta_0$ represents the torque angle and $X$ is the line impedance.

Figure 4.2 shows another scenario where there are perturbations at time instants 0.2 s and 0.3 s. The first perturbation commanded a power pulse of 30 MW which was beyond the stable operating level. The second perturbation was of a much smaller magnitude, 12 MW, which also was above the stable operating range. The lower graph is a plot of the energy function $V$, which is proposed as a Lyapunov-like function. Whenever the power is commanded beyond the normal operating limits, the system frequency will also shift and will no longer remain at the nominal operating point of 60 Hz. Hence as per (15), deviation of the frequency from the nominal level will cause an ensuing increase in the error of the energy function, which indicates potential instability. Thus as can be seen from Figure 4.2, the energy function rises at those two

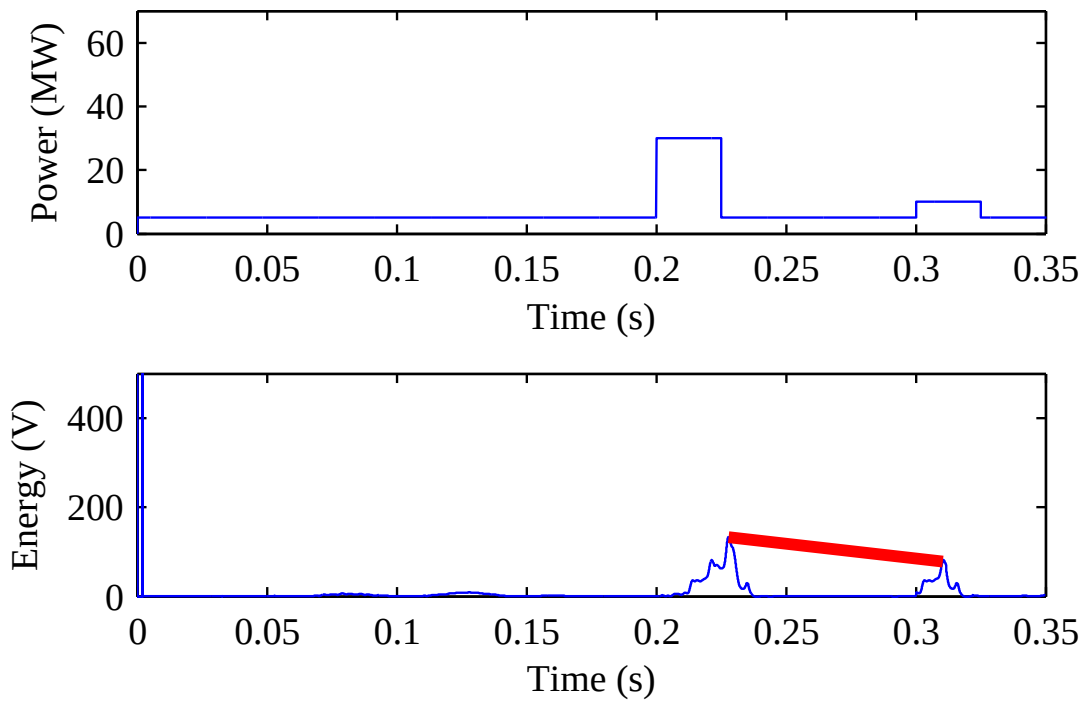


Figure 4.2. Simulated microgrid performance in response to commanded power pulse where system remains stable.

specific instants when the system is disturbed beyond its normal range of operation but eventually goes back to zero, indicating that the system had regained stability. Since the value of $V$ at successive switching instants decreases, $V$ is a Lyapunov-like function and the system is stable.

The next scenario is illustrated by Figure 4.3. The perturbation instants are the same as in the previous case and so is the magnitude of the first perturbation. However in this case the second perturbation is much higher (60 MW). Such a high disturbance does not allow the system to regain its stability which had been corroborated by the energy function plot of Figure 4.3. Since the value of $V$ at switching instants is not decreasing, the system may be unstable, and in this case indeed diverges from the desired operating point. The heavy red lines in Figures 4.2-4.3 indicate the increase or decrease in the energy function at subsequent switching instants.

Lyapunov-like functions for the present model were thus framed from the error in the energy function. It was seen that the behavior of Lyapunov-like functions for the

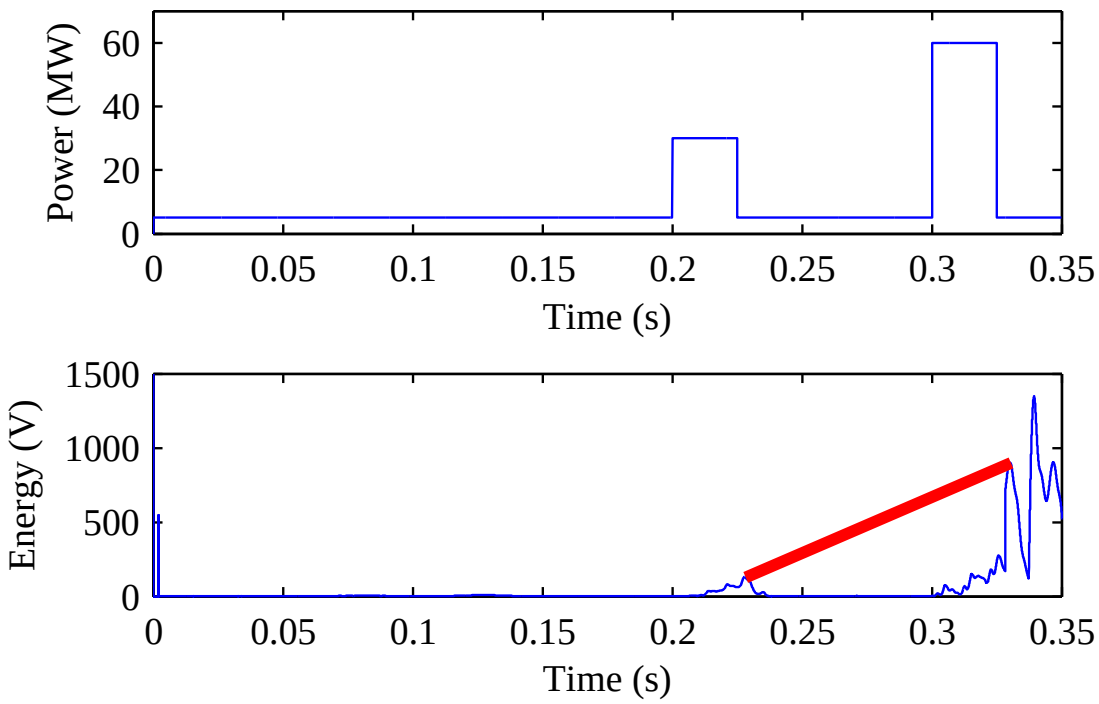


Figure 4.3. Simulated microgrid performance in response to commanded power pulse where system is unstable.

experimentally stable and unstable cases maintained conformity with the discussion on Lyapunov theory in Section 2. However Lyapunov-like functions are only way of determining the stability of a switched system.

The stability of the system can be captured in the frequency of the generator. For a perfectly stable system,the operating frequency should be at the nominal margin of 60 Hz or 376.8 rad/sec. However it will be interesting to study how the system operating frequency deviates from the nominal level in the possible event of a power imbalance. This opens up a whole new prospect of droop implemenation and invariant analysis which shall be dealt in the upcoming sections.

## 4.2. INTRODUCTION TO DROOP AND INVARIANT STUDIES

Let us go back to Figure 4.1 once again. As can be seen from Table 4.1, the power is balanced at the 1.0 second instant. Theoretically the system should go back to its nominal frequency level since there are no power imbalances to make the operating

frequency deviate from the nominal margin. However the graphical result shows that the system crashes after the 1.0 second instant. This is because although the power imbalance had been restored, there is factor missing which brings the system back to its stable operating level. This missing factor is a *droop constant*. Thus there is not enough droop in the system which explains why the system crashes even after the power mismatches are restored. Thus we need to introduce a certain amount of droop to the system so that the system returns back to its stable operating level when the power mismatches are restored. The invariant equation (13) expresses this minimum amount of droop needed to guarantee system stability. The accuracy of this theoretical equation shall be tested by conducting actual simulations. An acceptable conformity in results between this theoretical invariant prediction of system behavior and system behavior as interpreted from experimental simulations will justify the invariant equation. This has been studied in greater details in the next section

# 5. INVARIANT AND DROOP ANALYSIS EXPERIMENTS

A question that keeps coming back is what exactly is the role of this droop. The droop constant factor modifies $P$ based on $\omega$. It is a measure of stiffness of the system. Thus too high values of droop will make the system stiffer and we will not be able to observe anything interesting. However an insufficient droop will fail to provide the system with the required amount of stiffness it needs. The result may be a system crash similar to the one shown in Figure 4.1 which was a zero droop system.

From the invariant expression, it is possible to determine the critical value of $m$, provided that we have the appropriate values for the individual parameters in the expression. $D$ and $k$ are constants whose approximate values have been evaluated. Conducting experimental test cases on system stability helps us to find values of outstanding number of messages $K$, operating frequency $\omega$ and the gross power flow in the system $P$ to plug into the invariant expression. Thus with all known values, the system critical droop constant have been theoretically evaluated as $m$=0.572. This means for $m$ values less than this, the system will not be able to maintain stability even if there is no power imbalance.

In order to prove this theoretical assumption, an experimental test case was run with no power imbalance but $m$=0.57 which is slightly less than 0.572. Figure 5.1 depicts the system behavior for such a case when $m$ is 0.57 and $K$ is 0. It shows that the system is going unstable. Because of PSCAD® memory restrictions, it is not possible to run the simulation for more than 18 seconds which would have otherwise shown the system crashing. But from what can be seen within the limited time range, the system clearly shows tendencies of crashing. It can be safely concluded that in the absence of enough droop, the system will eventually crash but will take a long time to do so. If we want to see a case where the system does indeed crash within the permissible simulation time frame, we have to run an experiment with droop constant well below the critical droop constant value (say $m$=0.10). Figure 5.2 clearly shows that the system is crashing in the absence of sufficient droop.

An interesting alternative approach can be adopted from the invariant expression pertaining to the number of outstanding messages $K$. If $K$ value can be made

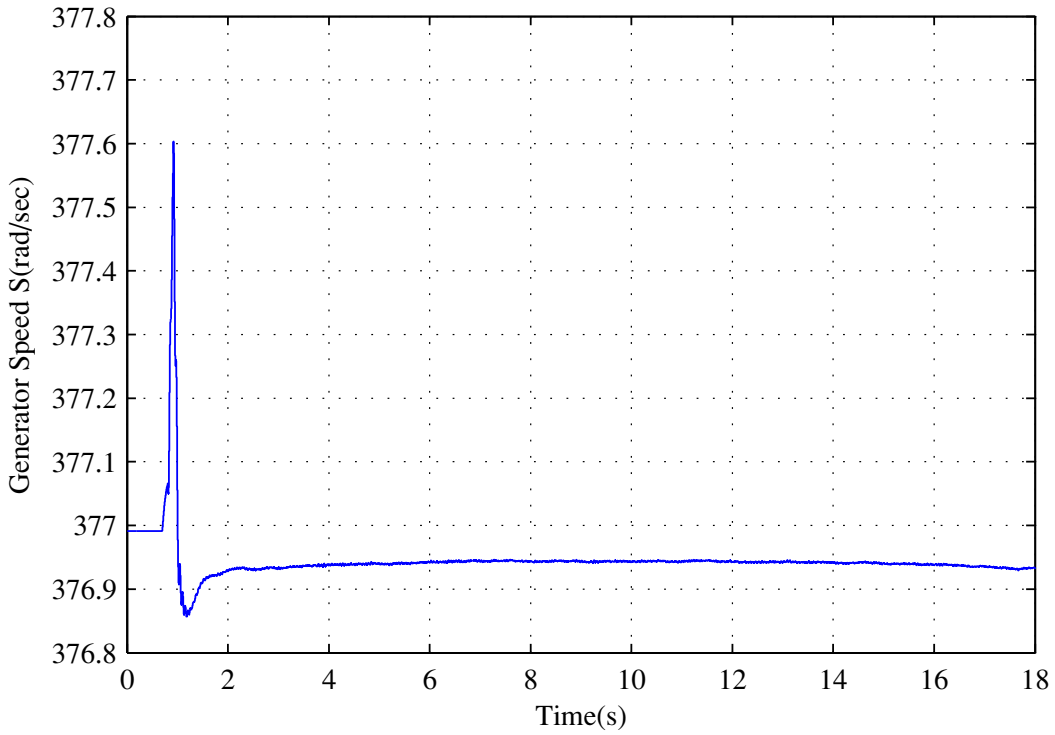


Figure 5.1. System behavior when $m$=0.57 and $K$=0

negative for Figure 5.1 where the droop constant was 0.57, even lower values of $m$ might suffice to make the system stable as long as $\omega - \omega_0$ remains non negative. This is purely a theoretical line of reasoning since the invariant formulation suggests that a negative value of $K$ makes the entire right hand side expression negative (provided that $\omega - \omega_0$ =0) and hence any non negative value of droop must be able to keep the system stable. With this theoretical hypothesis in mind, the experiment in Figure 5.1 was performed again with the same value of m but a different value of $K$ ($K$=-5). The graphical system behavior has been illustrated in Figure 5.3 . The system response shows that the variation in $K$ makes the system plunge lower than the earlier case (when $K$ was 0) at the time instant when the variation was enforced. However unlike the earlier case, the same value of droop constant guides the system back to its stable operating point.

As the simulations had been run to demonstrate system performance, the invariant was also tested. Table 5.1 can be formulated to show the relationship between invariant prediction and system response.

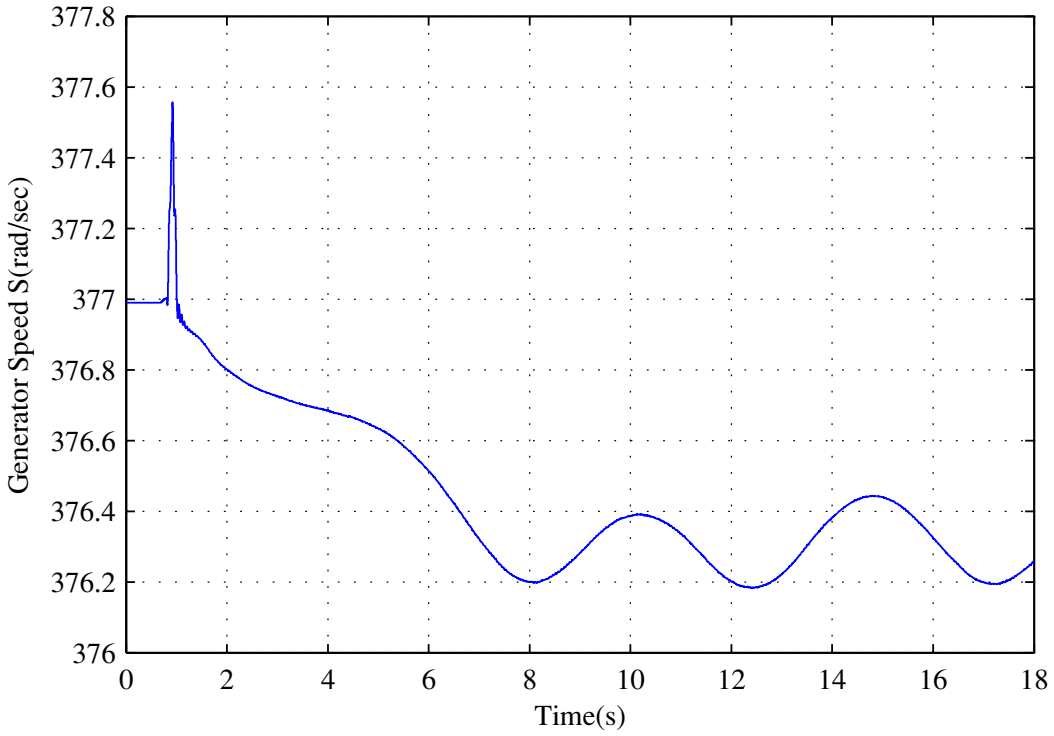


Figure 5.2. System behavior when $m$=0.10 and $K$=0

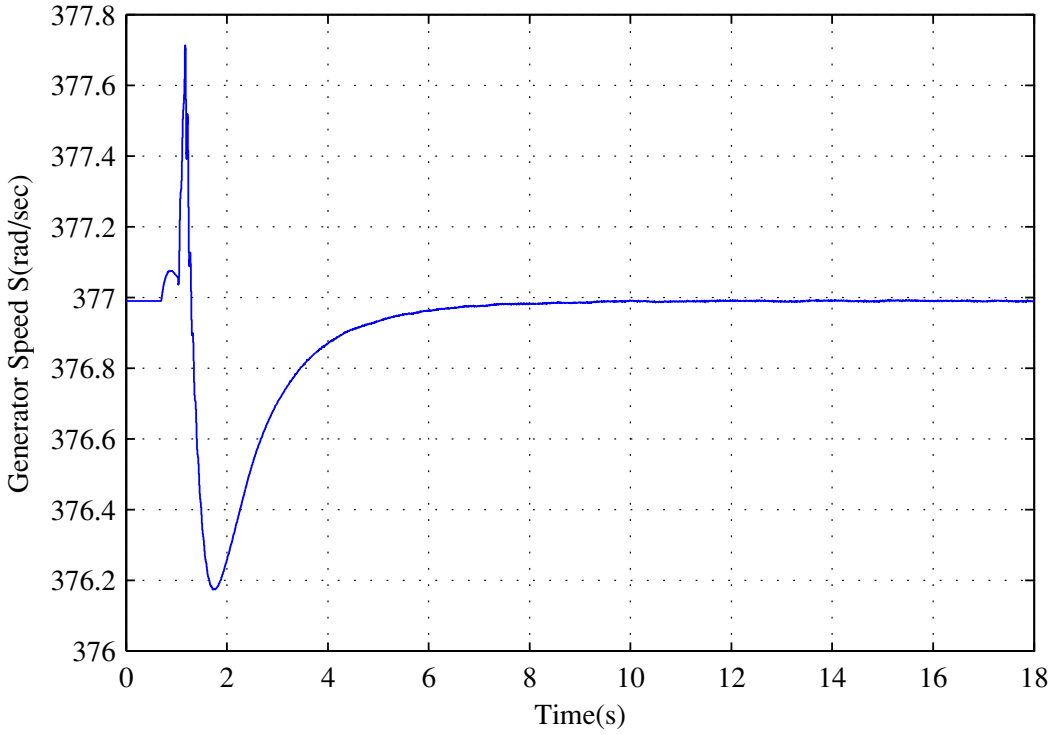


Figure 5.3. System behavior when $m$=0.57 and $K$=-5

Table 5.1. Relationship between Invariant Prediction and System Response for the first set of experiments.

| **K** | **m** | **Invariant Prediction** | **System Response** |
|---|---|---|---|
| 0 | 0.57 | Unstable | Unstable |
| 0 | 0.10 | Unstable | Unstable |
| -5 | 0.57 | Stable | Stable |

It is thus possible to play with the values of $m$ and $K$ and study the correlation between invariant prediction and system response. The following set of experiments deal with a constant negative value of $K$ while $m$ is varied.

## 5.1. INVARIANT AND SYSTEM RESPONSE FOR $K$=-10

This section explores cases when $K$ had been kept constant at -10 and the droop constant $m$ varied. Figure 5.4 describes the system response when $m$ =0.05 which is minimal droop. The second case has a droop constant value of 0.10 which is illustrated in Figure 5.5. Both these cases are instances of insufficient droop as a result of which it can be seen that the system crashes. The third instance as shown in Figure 5.6 shows a stable behavior although the droop constant is 0.50 and is actually less than the critical value of droop constant. But as can be recalled from earlier discussions, sometimes a negative value of $K$ has the power to make the system stable which is exactly the situation here. The invariant readily agrees to this logic because with $\omega$ being on the correct side of $\omega_0$, a negative $K$ renders the entire expression negative which is obviously less than the droop constant and hence adheres to the correct prediction of the system response as per the invariant theory. The fourth case has a droop constant value of 0.90 as shown in Figure 5.7. Figure 5.8 depicts the system response when $m$=1.20. As expected, these high values of droop constant guides the system back to stability as can be seen from the graphs.

Thus the experiments reported in this section with $K$=-10 and $m$ varying were in accordance with the invariant formulation. This can be shown in the form of Table 5.2 which again sums up the relationship between the invariant prediction and system response. The graphical plots and the table had also been shown.

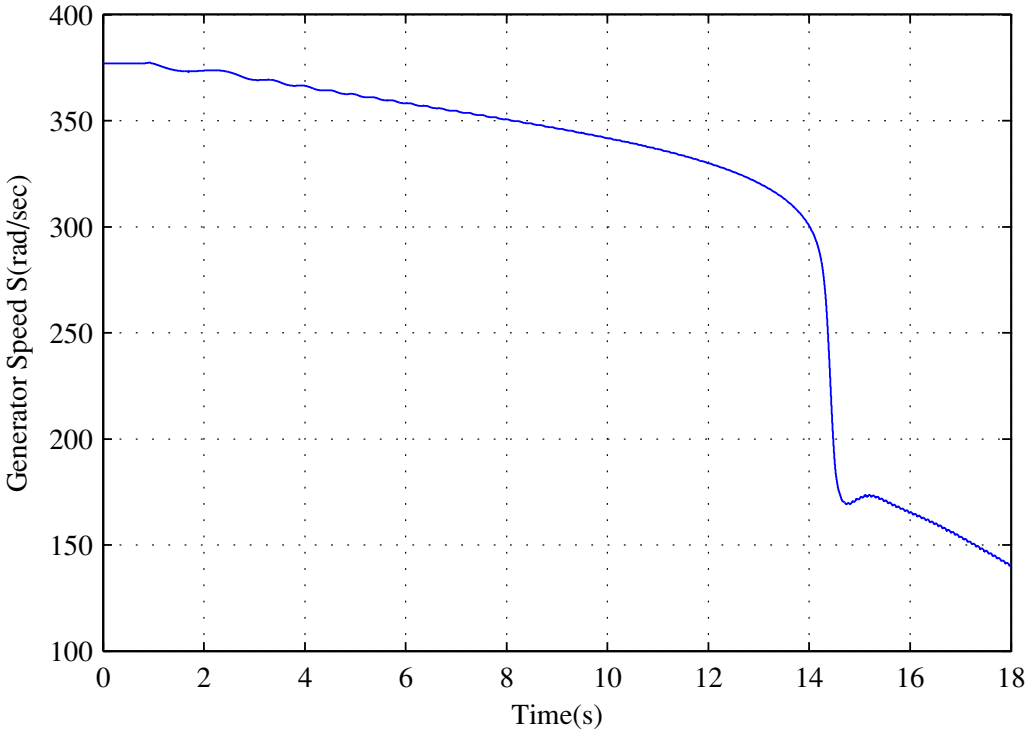


Figure 5.4. System behavior when $m$=0.01 and $K$=-10

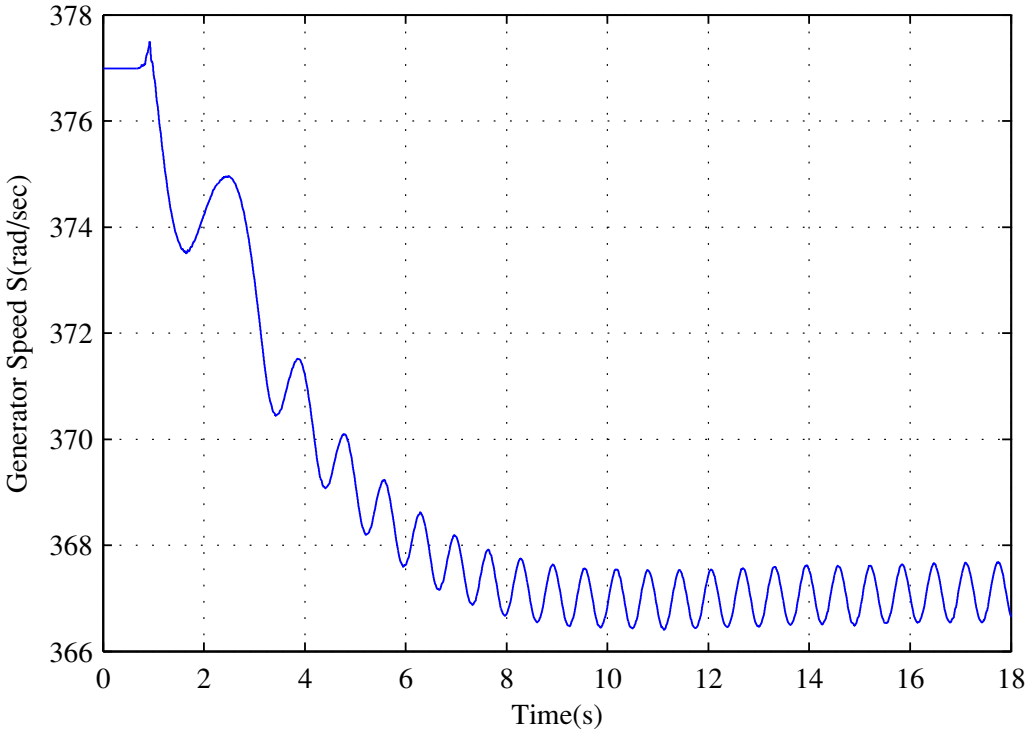


Figure 5.5. System behavior when $m$=0.10 and $K$=-10

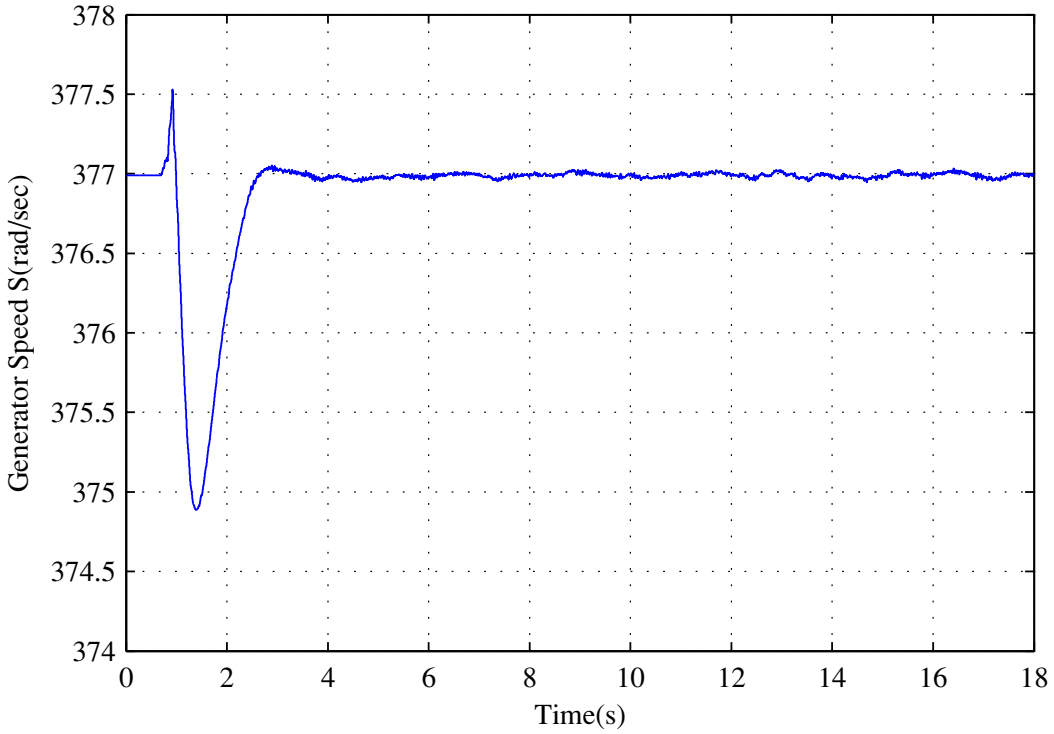


Figure 5.6. System behavior when $m$=0.50 and $K$=-10

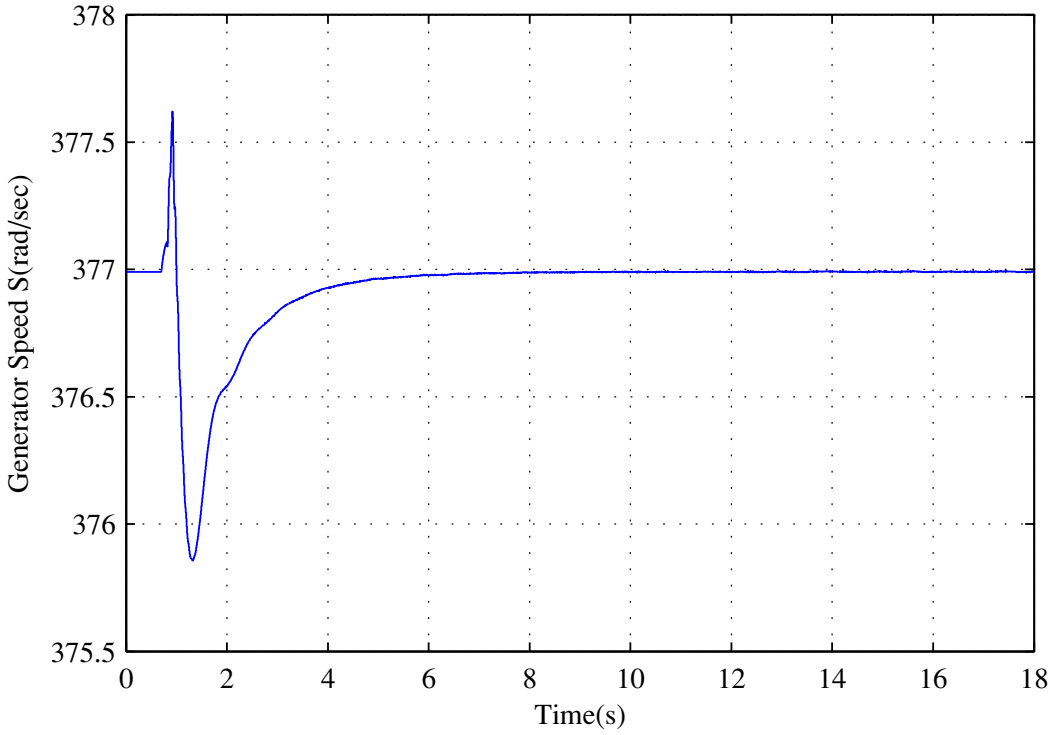


Figure 5.7. System behavior when $m$=0.90 and $K$=-10

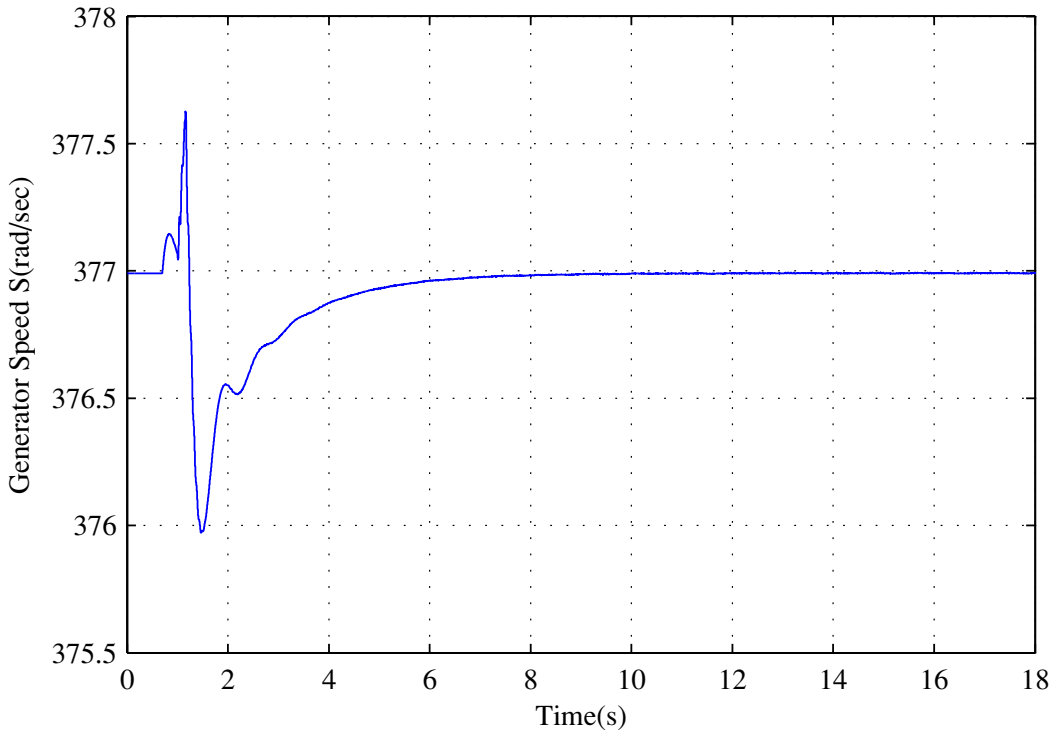


Figure 5.8. System behavior when $m$=1.20 and $K$=-10

Table 5.2. Relationship between Invariant Prediction and System Response for constant negative $K$ and varying $m$.

| **K** | **m** | **Invariant Prediction** | **System Response** |
|---|---|---|---|
| -10 | 0.01 | Unstable | Unstable |
| -10 | 0.10 | Unstable | Unstable |
| -10 | 0.50 | Stable | Stable |
| -10 | 0.90 | Stable | Stable |
| -10 | 1.20 | Stable | Stable |

## 5.2. CORRELATION STUDIES AT CONSTANT DROOP

In the earlier section , we discussed the effect of a constant negative $K$ on the system while $m$ was varied. This helped us kind of predict the range of $m$ around

which the system is stable. In this section we are going to show the reverse relationship. A number of experiments had been performed on the system at a constant droop constant. However for all of these experiments reported in this section, $K$ had been varied to observe the effect on the system stability. It is imperative to note what value of $K$ keeps the stable. Technically speaking, the system can only sustain a certain number of outstanding messages before going unstable. Thus this helps us to estimate the range of $K$ around which the system exhibits stable behavior.

**5.2.1. When Droop Constant is 0.85.** This section describes the system behavior when $m$ is maintained at 0.85. As mentioned above, the number of oustanding messages $K$ had been varied to study the system behavior. However for these experiments, the variable values of $K$ had always been chosen non-negative unlike the earlier section.

As reported in the experiments below, the critical value of $K$ that kept the system stable for this value of droop was K=25. A total of four experiments were conducted for this section out of which two were stable and two unstable. Special emphasis has been given when the system transitions from stable to unstable domain as the critical value of $K$ is surpassed.

Figure 5.9 and Figure 5.10 shows stable system responses for values of $K$=20 and $K$=25. Figure 5.11 is marginally stable when the critical value of K had just been violated at $K$=26. Figure 5.12 shows an unstable system response with the operating frequency showing sustained oscillations around the nominal frequency mark when $K$ is maintained at 30. These sustained oscillations get bigger in magnitude as values of $K$ are increased further. The graphical plots had been illustrated to show the system behavior. This clearly states that at that much amount of droop, the system can maintain its stable operation for values of $K$ no greater than 25.

Once again the invariant logic was applied to interpret system behavior and check if they conformed to the graphical responses as obtained from simulation results. Accordingly Table 5.3 shows the correlation between system behavior and invariant prediction. This table shows that system response and invariant prediction were in synchronism.

**5.2.2. When Droop Constant is 1.00.** This section studies the system response for unity value of droop constant while $K$ is varied. Again we need to keep a

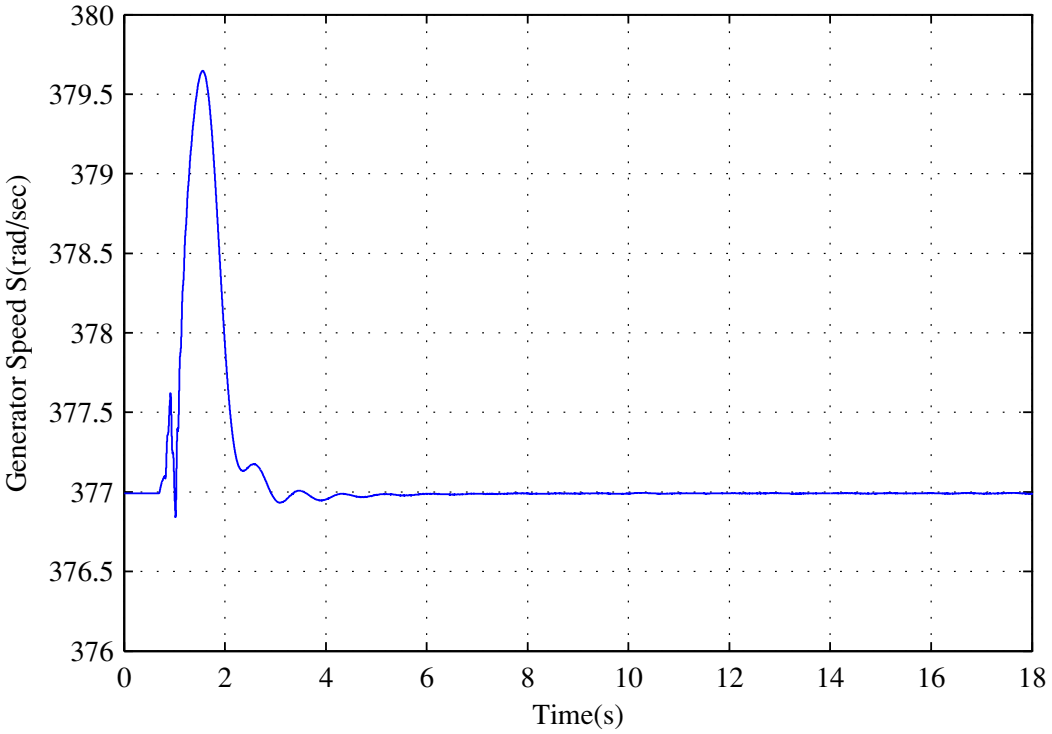


Figure 5.9. System behavior when $m$=0.85 and $K$=20

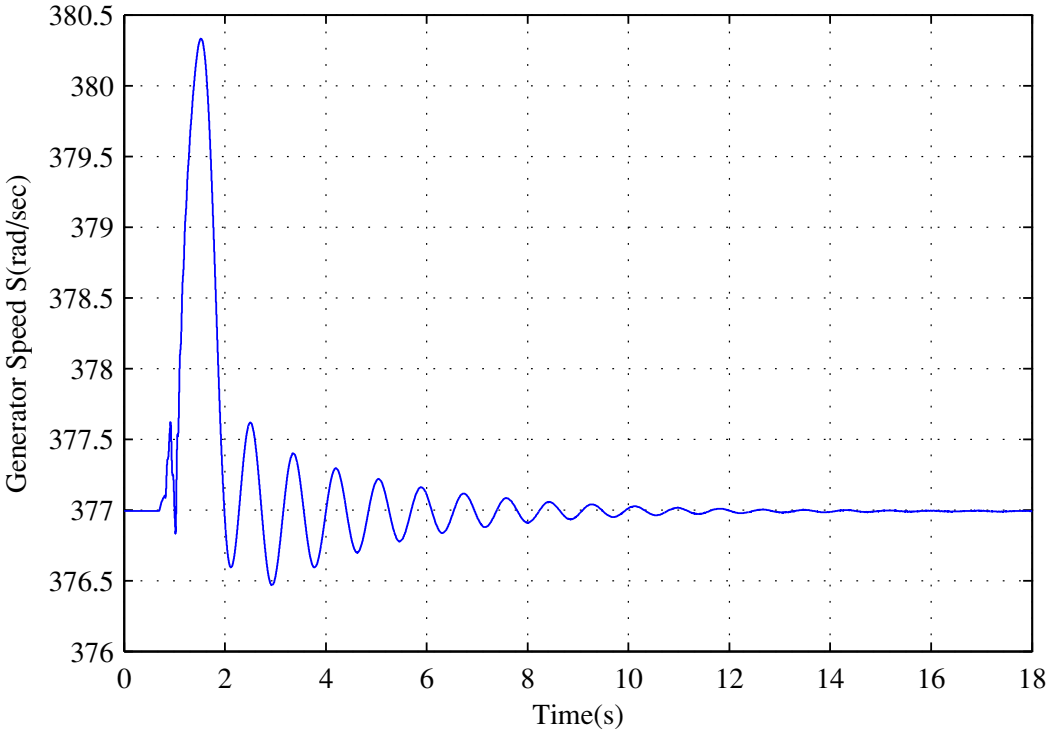


Figure 5.10. System behavior when $m$=0.85 and $K$=25

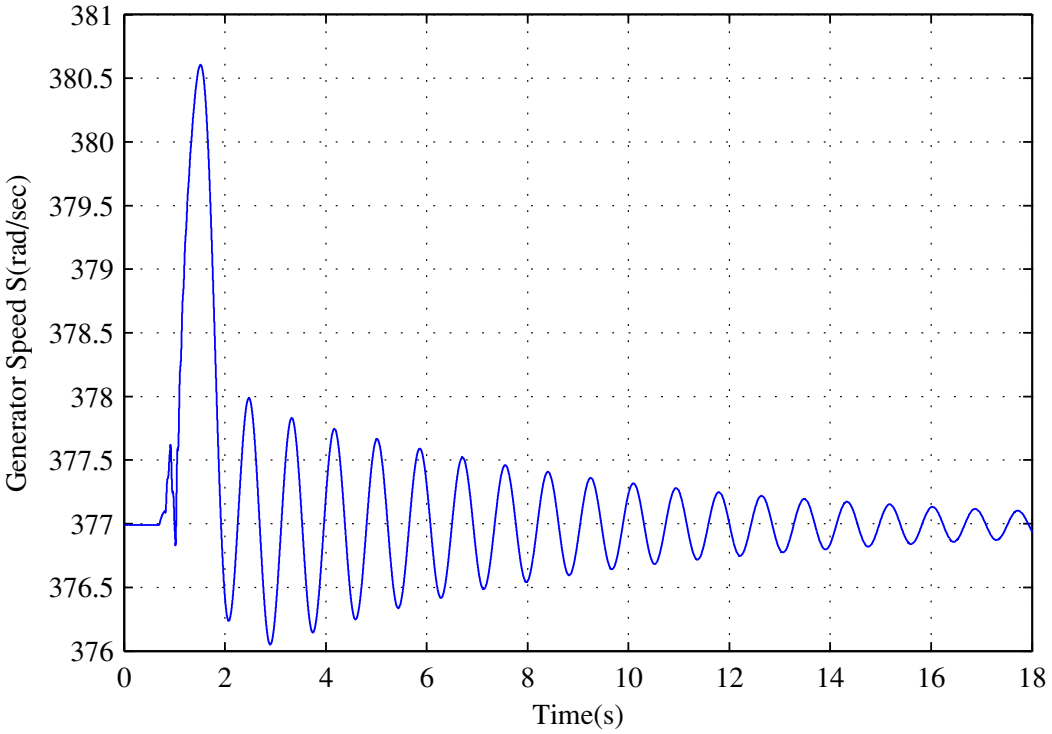


Figure 5.11. System behavior when $m$=0.85 and $K$=26

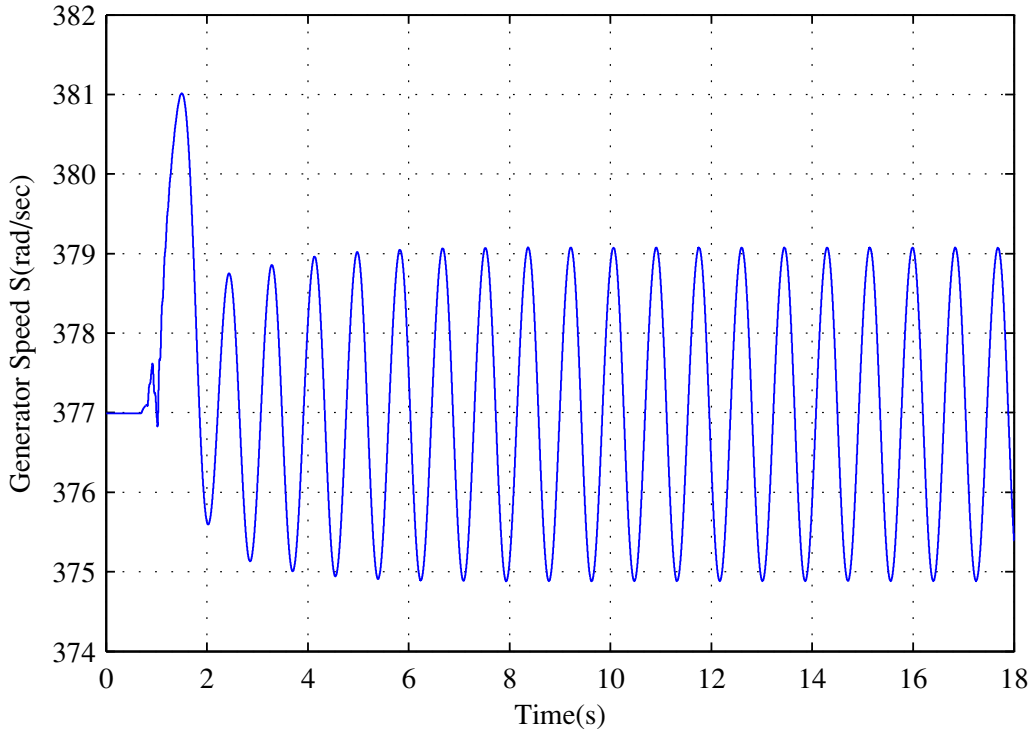


Figure 5.12. System behavior when $m$=0.85 and $K$=30

Table 5.3. Relationship between Invariant Prediction and System Response for $m$=0.85 and variable $K$

| **K** | **m** | **Invariant Prediction** | **System Response** |
|---|---|---|---|
| 20 | 0.85 | Stable | Stable |
| 25 | 0.85 | Stable | Stable |
| 26 | 0.85 | Unstable | Marginally Stable |
| 30 | 0.85 | Unstable | Unstable |

lookout for that value of $K$ beyond which the system goes unstable. Like the previous section, the system again went unstable when the number of outstanding messages exceeded 25.

Figure 5.13 and Figure 5.14 are stable case scenarios. Figure 5.15 is again a marginally stable condition when the critical value of K had just been passed. Figure 5.16 is an unstable condition as can be understood from the prominent oscillations. The invariant was again tested for all these cases. The results obtained from invariant prediction and actual system behavior has been compared in a tabular form as shown in Table 5.4.

An interesting observation based from the earlier two sections is that there is a significant change in system stability as the outstanding number of messages were increased. The most significant change is capturing the transition of the system from stable to unstable domain at the other side of $K$=25. An encouraging deduction is that the system response corroborated the invariant predictions for all the cases tested above. It is fascinating how the increase in $K$ affects the system dynamics so prominently.

Variation in droop constant values enable us to study very interesting dynamics of the system. When $m$=0.85, the transients were much elastic as compared to $m$=1.0. Thus it seems that increasing the droop constant value introduces an extra stiffness to the system which is exactly the very essence of droop. In this light, it should be mentioned that selecting too high values of droop is not advisable as it will make the system so stiff that no interesting dynamics can be observed. Thus a justifiable selection of the droop constant is important if we are to capture interesting results.

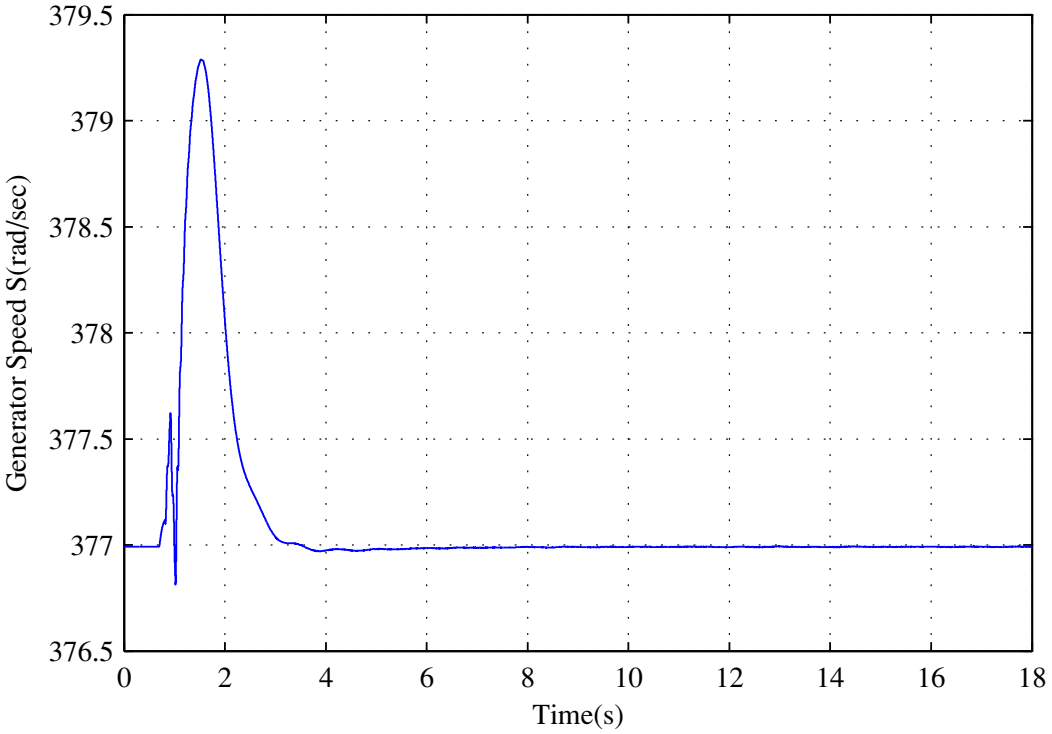


Figure 5.13. System behavior when $m$=1 and $K$=20

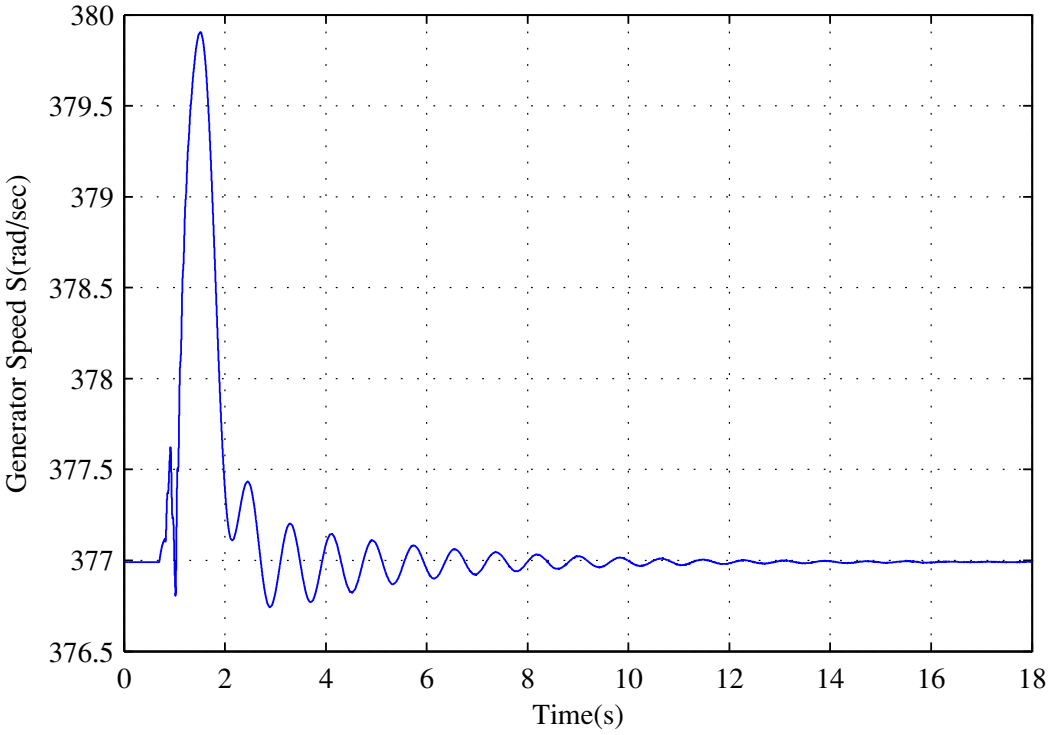


Figure 5.14. System behavior when $m$=1 and $K$=25

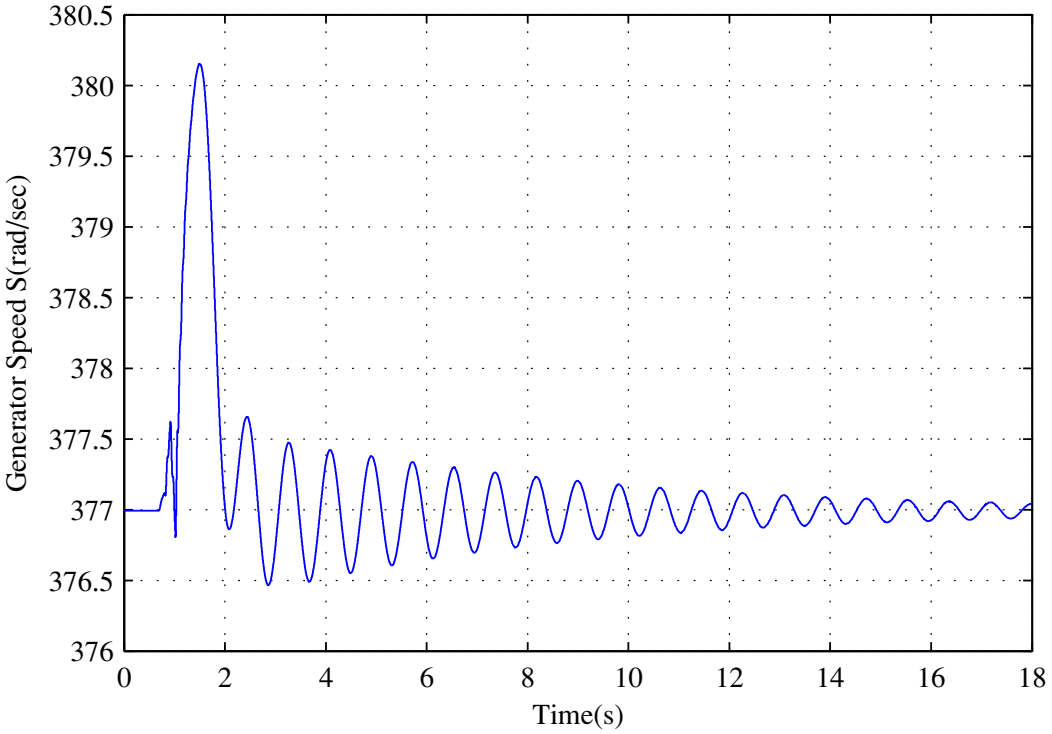


Figure 5.15. System behavior when $m$=1 and $K$=26

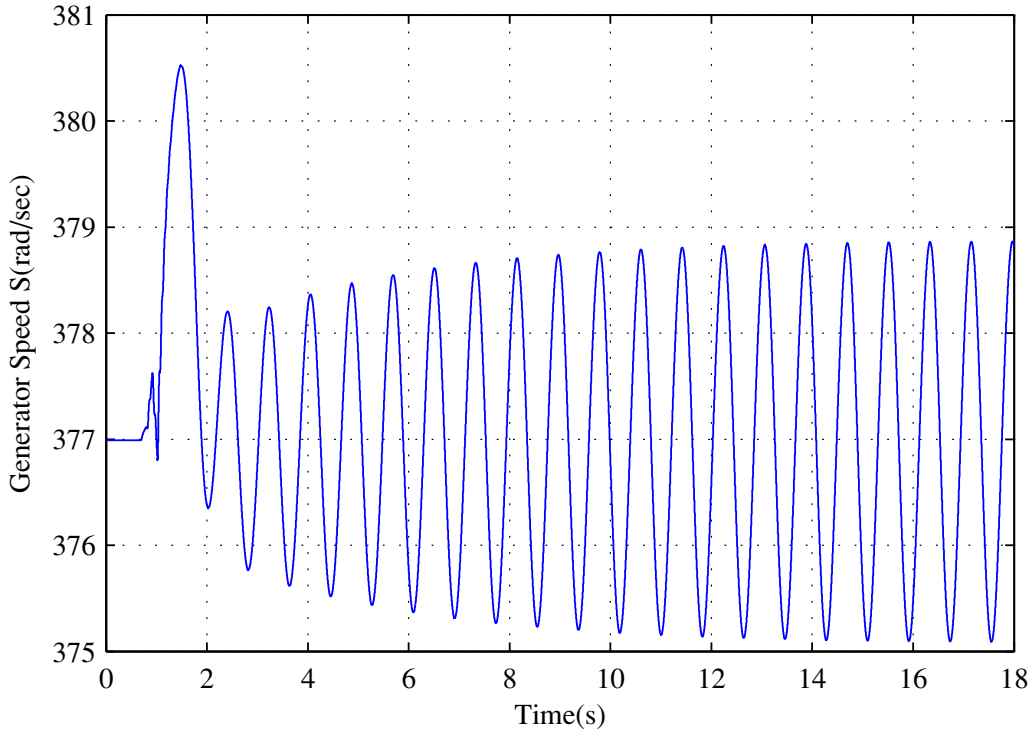


Figure 5.16. System behavior when $m$=1 and $K$=30

Table 5.4. Relationship between Invariant Prediction and System Response for $m$=1.00 and variable $K$

| **K** | **m** | **Invariant Prediction** | **System Response** |
|---|---|---|---|
| 20 | 1 | Stable | Stable |
| 25 | 1 | Stable | Stable |
| 26 | 1 | Unstable | Marginally Stable |
| 30 | 1 | Unstable | Unstable |

## 5.3. ADDITIONAL CASES STUDIED

In addition to the cases shown, several other experiments were also conducted. A summary of all the experimental test cases ran have been represented in Figure 5.17. The blue circles denote stable operation and red crosses indicate unstable operation as determined both by Invariant Prediction and Simulation Results.

## 5.4. ANALYSIS

This chapter primarily tests the accuracy of the invariant by running actual test case simulations. However a few things need to be mentioned. In any of the cases if the invariant predicts that the system is stable/unstable and the simulation responses also show that the system is stable/unstable, it adds strength to the invariant formulation. However if the invariant predicts that the system is unstable and the system turns out to be stable, it proves that that the invariant is a little conservative but it is acceptable nevertheless. But a weak invariant is not at all acceptable. This means a condition where the invariant predicts that the system is stable but the system turns out to be unstable.

In all the cases that had been reported, not a single event had been such that pertains to the *weak invariant* and hence the *bad* condition case. Thus it can be said that the invariant that we have developed is quite accurate in judging the system dynamics. The experiments conducted in this chapter also proves that it is possible to violate the invariant as well as the system stability by playing with the $K$ and $m$

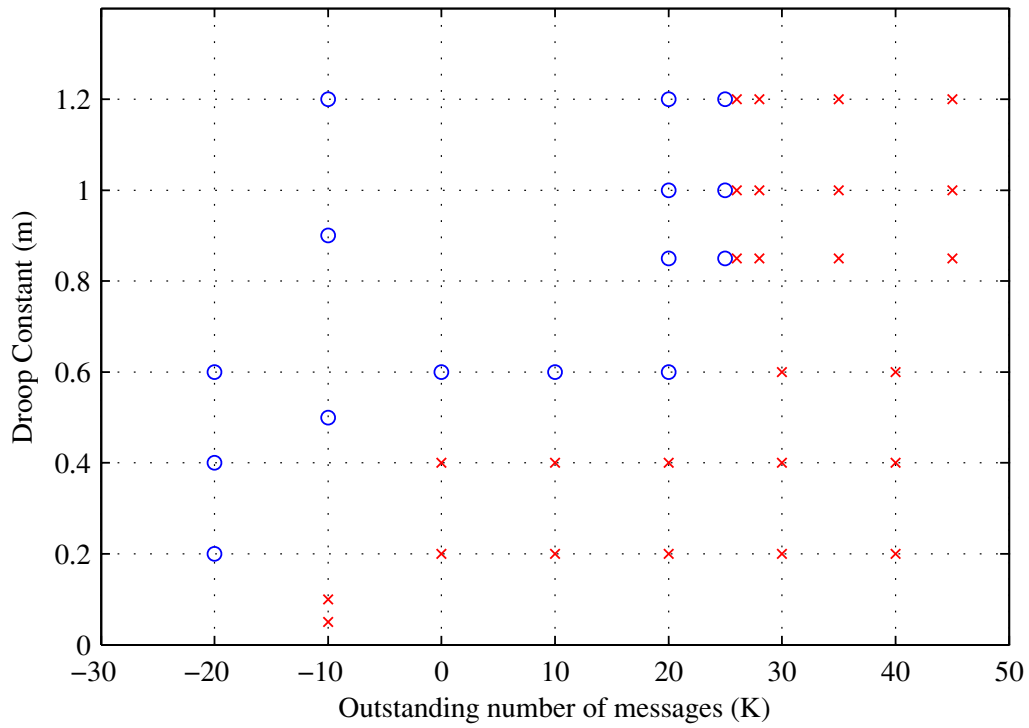


Figure 5.17. Simulated system behavior and truth value of invariant. Blue circles denote stable operation and red crosses indicate unstable operation as determined both by Invariant Prediction and Simulation Results.

parameters. These are the only two parameters that can be controlled since all other parameters are either constants or simulation dependant factors. Summing up, it can be said that with no backlog in message delivery ($K$=0), a droop constant value equal or higher than the critical droop constant value will maintain system stability. Again in certain cases, a negative $K$ assures stable system operation even though the droop constant might be below the critical value. Also for a certain specified droop but above the critical droop, the system remains stable upto a certain value of $K$. In other words, this means that the system can sustain only so many number of delayed power transactions before getting unstable at a certain droop. Thus it is possible to chalk out a stable zone of operation of the system for different values of $K$ and $m$ by conducting enough experiments on the system.

# 6. CONCLUSION AND FUTURE WORK

This thesis seeks to unify the knowledge present in the diverse areas of power and computing. The challenge is to provide a common semantic for these diverse areas by a unified treatment of invariants and noninterference of actions. Invariants are a natural fit to explain cyber systems. Lyapunov-like functions provide invariants for physical and network systems and noninterference is the glue that ties all three together.

A physical system was designed in the present study. A controllable Solid State Transformer (SST) model was implemented to carry out the stressed power migrations. Lyapunov-like functions were composed to describe the stability of the system. Simulations were carried out to demonstrate the Lyapunov-like behavior of a stable switched system and an unstable switched system. The system dynamics were studied and an invariant expression was proposed to describe the behavior of the system. This expression can be called the physical invariant of the system. To validate this invariant, simulations were carried out by varying the variable parameters in the invariant expression. Uniformity in theoretical analysis and simulation results proved the credibility of the invariant expression to explain the system dynamics.

While invariants are a naturally occurring artifact of formal cyber system specification, with Lyapunov functions, there are no generic tools that would enable system designers to find a Lyapunov-like function ($V$) for a given non linear switched system. The proposed approach used the energy of the error as the Lyapunov-like function for the given system. To extend the concept, the dynamics of $V$ need to be estimated over short time scales to determine how much $V$ changes between mode changes. Singular perturbation methods [37] enable the separation of the dynamics into "slow" and "fast" time scales to simplify the analysis. Future work can be done on studying the system behavior in response to switching values of $K$ thereby studing a dynamic response.

Correction of the system in the subsequent event of invariant violation is another issue. Droop is one corrective action, message backlog reduction, or stopping the power migration from one or more SSTs can improve the system stability. Further

investigation is required to explore more integrated cyber-physical-network corrective actions. The significant challenge is that any proposed correction must not interfere with the correctness of the system invariant.

# BIBLIOGRAPHY


[1] B. Manfred, "Challenges in automotive software engineering," in *Proceedings of the 28th international conference on Software engineering*, pp. 33–42, April 2006.

[2] T. Paul, J. W. Kimball, M. Zawodniok, T. P. Roth, and B. McMillin, "Invariants as a unified knowledge model for cyber-physical systems," in *IEEE International Conference on Service Oriented Computing and Applications (SOCA'11)*, International Workshop on Knowledge and Service Technology for Life, Environment, and Sustainability (KASTLES), December 2011.

[3] C.-T. Chen, *Linear System Theory and Design*. New York: Holt,Rinehart and Winston, 1985.

[4] D. Liberzon, *Switching in Systems and Control*. Boston: Birkhauser, 2003.

[5] D. L. Rajeev Alur, "A theory of timed automata," *Theoretical Computer Science*, vol. 126, no. 2, pp. 183–235, 2004.

[6] M. S.Branicky, "Multiple lyapunov functions and other analysis tools for switched and hybrid systems," *IEEE Transactions on Automatic Control*, vol. 43, no. 4, pp. 475–482, 1998.

[7] H. Ye, A. N. Michel, and L. Hou, "Stability analysis of systems with impulse effects," *IEEE Transactions on Automatic Control*, vol. 43, no. 12, pp. 1719–1723, 1998.

[8] H. Ye, A. N. Michel, and L. Hou, "Stability theory for hybrid dynamical systems," *IEEE Transactions on Automatic Control*, vol. 43, no. 4, pp. 461–474, 1998.

[9] Y. Zhu, E. Westbrook, J. Inoue, A. Chapoutot, C. Salama, M. Peralta, T. Martin, W. Taha, M. O'Malley, R. Cartwright, A. Ames, and R. Bhattacharya, "Mathematical equations as executable models of mechanical systems," in *Proceedings of the 1st ACM/IEEE International Conference on Cyber-Physical Systems*, ICCPS '10, (New York, NY, USA), pp. 1–11, ACM, 2010.

[10] M. Sintzoff and F. Geurts, "Analysis of dynamical systems using predicate transformers - attraction and composition," in *Analysis of Dynamical and Cognitive Systems*, pp. 227–260, 1993.

[11] "Incremental invariant generation for compositional design," Tech. Rep. TR-2010-6, Verimag Research Report, 2010.

[12] S. Owicki and D. Gries, "An axiomatic proof technique for parallel programs," *Acta Informatica*, vol. 6, pp. 319–340, 1976.

[13] C. A. R. Hoare, "An axiomatic basis for computer programming," *Communications of the ACM*, vol. 12, pp. 576–585, October 1969.

[14] T. H. Cormen, C. E. Leiserson, R. L. Rivest, and C. Stein, *Introduction to Algorithms*. Cambridge, MA: MIT Press, second ed., 2001.

[15] M. Roozbehani, M. Dahleh, and S. Mitter, "Robust and distributed decisions for future cyber-physical energy networks," June 2009.

[16] L.Massouli, "Structural properties of proportional fairness:stability and insensitivity," *Ann.Appli.Probab*, vol. 17, no. 3, pp. 809–839, 2007.

[17] S. M.Zawodniok, "Predictive congestion control protocol for wireless sensors," *IEEE Transactions on Wireless Communications*, vol. 6, no. 11, pp. 3955–3963, 2007.

[18] S.Jagannathan in *Wireless ad hoc sensor networks:protocols,performance,and control*, 2007.

[19] Y. Sun, B. McMillin, X. F. Liu, and D. Cape, "Verifying Noninterference in a Cyber-Physical System: The Advanced Electric Power Grid," in *Proceedings of the Seventh International Conference on Quality Software (QSIC)*, (Portland, OR), October 2007.

[20] A. Q. Huang, M. L. Crow, G. T. Heydt, J. P. Zheng, and S. J. Dale, "The Future Renewable Electric Energy Delivery and Management (FREEDM) System: The energy internet," *Proceedings of the IEEE*, vol. 99, pp. 133–148, Jan. 2011.

[21] R. Akella, F. Meng, D. Ditch, B. McMillin, and M. Crow, "Distributed power balancing for the FREEDM system," in *Smart Grid Communications (SmartGridComm), 2010 First IEEE International Conference on*, pp. 7 –12, October 2010.

[22] G. Levin and D. Gries, "A proof technique for communicating sequential processes," *Acta Inf.*, vol. 15, pp. 281–302, 1981.

[23] C.Hoare, *Communicating Sequential Processes*. Prentice Hall, 1985.

[24] S. G. Nersesov and W. M. Haddad, "On the stability and control of nonlinear dynamical systems via vector lyapunov functions," *IEEE Transactions on Automatic Control*, vol. 51, pp. 203–215, February 2006.

[25] S. Sathananthan and L. H. Keel, "Optimal practical stabilization and controllability of systems with markovian jumps," *Nonlinear Analysis*, vol. 54, pp. 1011–1027, September 2003.

[26] A. Morse., "Supervisory control of families of linear set point controllers-part1:exact matching," *IEEE Transactions on Automatic Control*, vol. 41, pp. 1413–1431, October 1996.

[27] P. Kokotovic, H. Khalil, and J. Reily, *Singular Perturbation Methods in Control:Analysis and Design*. London: Academic press, 1986.

[28] A.-G. Wu, G. Feng, G.-R. Duan, and H. Gao, "A stabilizing slow-switching law for switched discrete-time linear systems," in *Intelligent Control (ISIC), 2010 IEEE International Symposium on*, pp. 2099 –2104, Sept. 2010.

[29] A.-G. Wu, G. Feng, and X. Zeng, "State feedback stabilizing switching strategies with dwell time for switched discrete-time linear systems," in *Intelligent Control and Automation (WCICA), 2010 8th World Congress on*, pp. 975 –980, July 2010.

[30] Z. Sun, "Stabilizability and insensitivity of switched linear systems," *Automatic Control, IEEE Transactions on*, vol. 49, pp. 1133 – 1137, July 2004.

[31] F. Long, C. Cui, and C. Li, "Robust control for a class of uncertain switched systems," in *Fuzzy Systems and Knowledge Discovery, 2008. FSKD '08. Fifth International Conference on*, vol. 5, pp. 110 –114, Oct. 2008.

[32] J. Yepez, C. Lozoya, M. Velasco, P. Marti, and J. Fuertes, "Preliminary approach to lyapunov sampling in can-based networked control systems," in *Industrial Electronics, 2009. IECON '09. 35th Annual Conference of IEEE*, pp. 3033 – 3038, Nov. 2009.

[33] S. Bak, A. Greer, and S. Mitra, "Hybrid cyberphysical system verification with simplex using discrete abstractions," in *Real-Time and Embedded Technology and Applications Symposium (RTAS), 2010 16th IEEE*, pp. 143 –152, April 2010.

[34] L. Sha, "Using simplicity to control complexity," *Software, IEEE*, vol. 18, pp. 20 –28, July/Aug 2001.

[35] H. Akagi, Y. Kanazawa, and A. Nabae, "Instantaneous reactive power compensators comprising switching devices without energy storage components," *IEEE Transactions on Industry Applications*, vol. IA-20, pp. 625–630, May/June 1984.

[36] L. M. Ni, C.-W. Xu, and T. B. Gendreau, "A Distributed Drafting Algorithm for Load Balancing," *IEEE Transactions on Software Engineering*, vol. 11, pp. 1153–1161, 1985.

[37] J. W. Kimball and P. T. Krein, "Singular perturbation theory for dc-dc converters and application to pfc converters," *IEEE Transactions on Power Electronics*, vol. 23, pp. 2970–2981, November 2008.

# VITA

Tamal Paul was born in Kolkata, India. He received his Bachelor's degree in Electrical Engineering from National Institute of Technology, Durgapur, India in May 2010. He joined Missouri University of Science and Technology (formerly University of Missouri- Rolla) in Fall 2010 for his Masters Degree. He received his Masters degree in Electrical Engineering in May 2012 from Missouri University of Science and Technology, Rolla, Missouri.